

Convergent evolution on oceanic islands: comparative genomics reveals species-specific processes in birds

María Recuerda¹, Julio César Hernández Montoya², Guillermo Blanco¹, and Borja Milá³

¹National Museum of Natural Sciences

²Grupo de Ecología y Conservación de Islas, A. C.,

³Museo Nacional de Ciencias Naturales

March 12, 2024

Abstract

Understanding the factors driving phenotypic and genomic differentiation of insular populations is of major interest to gain insight into the speciation process. Comparing patterns across different insular taxa subjected to similar selective pressures upon colonizing oceanic islands provides the opportunity to study parallel evolution and identify shared patterns in their genomic landscapes of differentiation. We selected four species of passerine birds (common chaffinch *Fringilla coelebs/canariensis*, red-billed croucher *Pyrrhonorax pyrrhonorax*, house finch *Haemorhous mexicanus* and dark-eyed/island junco *Junco hyemalis/insularis*) that have both mainland and insular populations. For each species, we sequenced whole genomes from mainland and insular individuals to infer their demographic history, characterize their genomic differentiation, and identify the factors shaping them. We estimated the relative (F_{ST}) and absolute (d_{xy}) differentiation, nucleotide diversity (π), Tajima's D, gene density and recombination rate. We also searched for selective sweeps and chromosomal inversions along the genome. Changes in body size between island and mainland were consistent with the island rule. All species shared a marked reduction in effective population size (N_e) upon island colonization. We found highly differentiated genomic regions in all four species, suggesting the role of selection in island-mainland differentiation, yet the lack of congruence in the location of these regions indicates that each species adapted to insular environments differently. Our results suggest that the genomic mechanisms involved, which include selective sweeps, chromosomal inversions, and historical factors like recurrent selection, differ in each species despite the highly conserved structure of avian genomes and the similar selective factors involved.

1 **Convergent evolution on oceanic islands: comparative genomics reveals species-specific processes in**
2 **birds**

3
4 María Recuerda ^{1,2}, Julio César Hernández Montoya ³, Guillermo Blanco ¹, Borja Milá ¹

5 ¹ National Museum of Natural Sciences, Spanish National Research Council (CSIC), Madrid 28006, Spain.

6 ² Cornell Laboratory of Ornithology, Cornell University, Ithaca, NY, USA

7 ³ Grupo de Ecología y Conservación de Islas, A. C., Ensenada, Baja California, México

8
9

10

11 Corresponding authors: María Recuerda, Cornell Laboratory of Ornithology, Cornell University, Ithaca,
12 NY, USA, Email: mariarecuercacarrasco@gmail.com; and Borja Milá, Museo Nacional de Ciencias
13 Naturales, Calle José Gutiérrez Abascal 2, Madrid 28006, Spain; Tel. +34 914111328, Email:
14 b.mila@csic.es

15

16

17 ORCID numbers:

18 María Recuerda: 0000-0001-9647-3627

19 Julio César Hernández Montoya: 0000-0001-9703-8491

20 Guillermo Blanco: 0000-0001-5742-4929

21 Borja Milá: 0000-0002-6446-0079

22 Declarations of interest: none

23 **Abstract**

24 Understanding the factors driving phenotypic and genomic differentiation of insular populations is of
25 major interest to gain insight into the speciation process. Comparing patterns across different insular
26 taxa subjected to similar selective pressures upon colonizing oceanic islands provides the opportunity to
27 study parallel evolution and identify shared patterns in their genomic landscapes of differentiation. We
28 selected four species of passerine birds (common chaffinch *Fringilla coelebs/canariensis*, red-billed
29 crounch *Pyrrhocorax pyrrhocorax*, house finch *Haemorhous mexicanus* and dark-eyed/island junco *Junco*
30 *hyemalis/insularis*) that have both mainland and insular populations. For each species, we sequenced
31 whole genomes from mainland and insular individuals to infer their demographic history, characterize
32 their genomic differentiation, and identify the factors shaping them. We estimated the relative (F_{ST}) and
33 absolute (d_{xy}) differentiation, nucleotide diversity (π), Tajima's D, gene density and recombination rate.
34 We also searched for selective sweeps and chromosomal inversions along the genome. Changes in body
35 size between island and mainland were consistent with the island rule. All species shared a marked
36 reduction in effective population size (N_e) upon island colonization. We found highly differentiated
37 genomic regions in all four species, suggesting the role of selection in island-mainland differentiation,
38 yet the lack of congruence in the location of these regions indicates that each species adapted to insular
39 environments differently. Our results suggest that the genomic mechanisms involved, which include
40 selective sweeps, chromosomal inversions, and historical factors like recurrent selection, differ in each
41 species despite the highly conserved structure of avian genomes and the similar selective factors
42 involved.

43

44

45 **Keywords:** Comparative genomics, island rule, parallel evolution, speciation.

46 **Introduction**

47 The colonization of oceanic islands by mainland individuals has been a major engine of biological
48 diversification, resulting in the evolution of thousands of new species across the world (Schluter, 2000;
49 Grant, 2001; Price, 2008; Warren et al., 2015; Gillespie et al., 2020). These colonization events have also
50 provided valuable research models to study processes like evolutionary divergence and local adaptation
51 (Grant & Grant, 2002; Losos & Ricklefs, 2009; Brown et al., 2013). Upon colonization of oceanic islands,
52 individuals across taxonomic groups have often been subjected to similar demographic and selective
53 factors, like population bottlenecks, strong selection for local adaptation, and reduced dispersal (Woolfit
54 & Bromham, 2005; Whittaker et al., 2017). Shared patterns of phenotypic evolution of insular
55 populations across taxonomic groups has led to general biogeographic rules, like Foster's rule, also
56 known as the "island rule", which postulates that on islands small animals tend to become larger, and
57 large animals tend to become smaller (Foster, 1964; Clegg & Owens, 2002; Benítez-López et al., 2021).
58 These patterns suggest the possibility of parallel evolution across species, and provide the opportunity
59 to test whether the selective mechanisms acting during island colonization are shared across species,
60 and whether selection acts on the same or different genomic loci.

61
62 The genomic underpinnings of divergence in oceanic islands are poorly understood, yet an increasing
63 number of studies are addressing this topic thanks to the recent advances in high-throughput DNA
64 sequencing (reviewed in Sackton & Clark, 2019). Both selection and drift can drive phenotypic changes
65 in islands, yet patterns of parallel phenotypic change are more likely to be driven by selection than by
66 random drift (Clegg, 2009; Rosenblum et al., 2014). Parallel phenotypic changes on islands could be
67 promoted by similar selective pressures due to their particular features relative to the mainland, such as
68 simplified ecosystems, reduced trophic resources, the availability of new ecological niches, a reduction
69 in predation which often leads to an increase in intraspecific competition, and a reduction in
70 interspecific competition (Blondel, 2000; Losos & Ricklefs, 2009). These insular selective pressures
71 usually result in predictable changes in body size (Benítez-López et al., 2021), usually attributed to the
72 absence of predators and the shifts in competition, and also result in diet shifts in order to adapt to the
73 new trophic resources, leading to behavioral (Sayol et al., 2018; Lapiedra et al., 2021), morphological
74 (Glor et al., 2004; Campana et al., 2020) and physiological adaptations (Blanco et al., 2014; Tattersall et
75 al., 2018). The molecular basis of convergent phenotypic traits across species could be entirely species-
76 specific, or instead show evolutionary convergence among species. The degree of molecular parallelism
77 can range from sharing the same mutation on the same gene, to changes at different nucleotides within

78 the same gene, to changes in different genes within the same pathway (Manceau et al., 2010; Sackton &
79 Clark, 2019). The probability of molecular parallelism is determined by several factors, increasing when
80 selective pressures are similar and genomic constraints such as demography and phylogenetic history
81 are shared (Rosenblum et al., 2014). The genetic basis of the phenotypic traits under selection is also
82 important: single-locus traits have been often involved in repeated convergent evolution (e.g., Reed et
83 al., 2011; Colosimo et al., 2005), yet for polygenic traits, which can be modified through multiple
84 pathways, molecular parallelism becomes less likely (Rosenblum et al., 2014; Boyle et al., 2017, Sendell-
85 Price et al. 2021) resulting instead in heterogeneous, species-specific patterns of differentiation.

86
87 Understanding the factors that generate heterogeneous patterns of differentiation across the genome is
88 one of the main goals of population genomics (Cruickshank & Hahn, 2014; Burri, 2017; Ravinet et al.,
89 2017; Feng et al., 2020; Chase et al., 2021). The main factors shaping differentiation patterns are drift
90 and selection, but demographic history and genomic features such as recombination rate and gene
91 content also affect the distribution of the differentiated regions (Ravinet et al., 2017). Recent advances
92 in sequencing technologies have allowed studying the genomic landscapes of variation, which show the
93 distributional pattern of genomic variation across the entire genome (Ellegren et al., 2012; Nadeau et
94 al., 2012; Poelstra et al., 2014; Meier et al., 2018). When comparing differentiated populations, regions
95 that are highly divergent relative to the genomic background are known as “islands of differentiation”
96 (Turner et al., 2005; Ellegren et al., 2012) and are usually detected as regions of high relative divergence
97 (F_{ST} , Weir & Cockerham, 1984). Early genome scans interpreted F_{ST} peaks as signatures of strong
98 selection surrounded by valleys homogenized by gene flow (Nosil et al., 2009), where those F_{ST} peaks
99 were caused by marked differences in allele frequencies at locally adapted sites and the neutral loci
100 linked to them (Charlesworth et al., 1997; Feder & Nosil, 2010). However, when considering patterns of
101 absolute divergence (d_{xy}) and within-population diversity (π) besides F_{ST} , new interpretations of how
102 these islands of differentiation originate have been put forward. F_{ST} peaks could also appear when
103 population diversity is low in either of the populations compared, while d_{xy} is less affected by this
104 pattern. Several processes such as positive and/or background selection can reduce within population
105 nucleotide diversity and generate “islands” of relative divergence, while absolute divergence remains
106 unchanged (Cruickshank & Hahn, 2014; Burri et al., 2015; Irwin et al., 2018). Four models have been
107 proposed to explain the underlying cause of islands of differentiation (Irwin et al., 2016; Irwin et al.,
108 2018) and in order to differentiate these models it is crucial to understand the relationship between F_{ST} ,
109 d_{xy} and π (Cruickshank & Hahn, 2014; Irwin et al., 2016; Han et al., 2017; Irwin et al., 2018). Two of those

110 models account for speciation in the presence of gene flow (“divergence-with-gene-flow” and “sweep-
111 before-differentiation”) and the other two involve allopatric speciation (“Selection in allopatry” and
112 “Recurrent selection”) (Irwin et al., 2016). Moreover, other factors such as demographic history,
113 mutation rate heterogeneity, and recombination rate across the genome, as well as gene density, could
114 modify the genomic landscape (Ravinet et al., 2017). Therefore, to correctly interpret the genomic
115 landscapes of differentiation it is important to understand the demographic and evolutionary history of
116 the target taxa (Ravinet et al., 2017). Variations in effective population size (N_e) can produce different
117 genomic signatures. For instance, marked reductions in N_e such as those caused by population
118 bottlenecks at founder events, can modify levels of background selection and therefore the baseline for
119 the detection of outlier loci (Ferchaud & Hansen, 2016; Leroy et al., 2021).

120

121 Covariation of genomic patterns of differentiation among different avian species has been shown across
122 broad evolutionary timescales (Van Doren et al., 2017; Delmore et al., 2018; Vijay et al., 2017, Carbeck
123 et al., 2023) and the coincident location of differentiation peaks has been of special interest to
124 understand the process of convergent molecular evolution where similar loci evolve independently in
125 several species (Seehausen et al., 2014). Bird genomes show high synteny (Zhang, 2014), a relatively
126 stable number of chromosomes (Ellegren, 2010), similar recombination landscapes (Singhal et al., 2015;
127 Kawakami et al., 2017), and across species microchromosomes show higher density in gene content
128 than macrochromosomes (Dutoit et al., 2017; Singhal et al., 2015). The similarity in genomic landscapes
129 of differentiation across closely related and diverged avian species could be due to the non-random
130 distribution of gene content across the genome and the coincidence of low recombination areas along
131 with linked selection (Van Doren et al., 2017; Irwin et al., 2018), since it has been shown that the
132 recombination landscape in birds can be maintained across species over long evolutionary time periods
133 (Singhal et al., 2015).

134

135 Here we use a comparative approach to examine patterns of genome-wide differentiation in avian
136 species that have colonized oceanic islands, with the goal of assessing the relative roles of demographic
137 history, time of divergence, and directional selection in driving divergence and potentially evolutionary
138 convergence upon island colonization. We selected four passerine species that have mainland
139 populations and have also colonized oceanic islands; two species from mainland Europe that have
140 colonized the island of La Palma in the Canary Islands, Atlantic Ocean, the common chaffinch (*Fringilla*
141 *coelebs/canariensis*) and the red-billed chough (*Pyrrhonorax pyrrhonorax*), and two species from North

142 America that have colonized Guadalupe Island on the Pacific Ocean, the house finch (*Haemorhous*
143 *mexicanus*) and the dark-eyed junco (*Junco hyemalis/insularis*). The red-billed chough and the house
144 finch have diverged from mainland populations within the last 100,000 years, whereas the common
145 chaffinch and the junco have been separated from their mainland relatives for over 500,000 years
146 (Aleixandre et al., 2013; Morinha et al., 2020; Recuerda et al., 2021). Given that all four species have
147 colonized oceanic islands and have been subjected to potentially similar selective pressures, we first
148 analyzed if the differences phenotype between insular and mainland counterparts affected the same
149 traits across species. Changes in morphological traits are expected upon colonization of the new insular
150 environment (Warren et al., 2015; Whittaker et al., 2017) and those changes are likely to generate
151 detectable genomic signatures. Therefore, we also asked if the genomic landscapes of differentiation
152 are similar among species when taking divergence time into account.

153
154 We performed whole-genome resequencing of 9-12 individuals per treatment per species in order to
155 determine whether the four species showed similar patterns of differentiation in their genomic
156 landscapes, and whether these patterns have been shaped by similar processes. We studied the
157 demographic history and performed genomic scans of F_{ST} , d_{xy} , π , Tajima's D, recombination rate, gene
158 content and selective sweeps. We also scanned the genomes looking for putative chromosomal
159 inversions, which have been shown to underlie major phenotypic polymorphisms in birds (Tuttle et al.,
160 2016). We detected regions under selection among insular and mainland counterparts as F_{ST} outliers and
161 selective sweeps, and identified shared candidate genes among the four species. Comparing the
162 genomic signatures of island colonization in four different species that have been exposed to similar
163 selective pressures and that differ in colonization time (which can be considered as a proxy for different
164 stages along the speciation continuum), can provide useful understanding for the mechanisms shaping
165 the genomic landscapes through the divergence process over time.

166

167 **Methods**

168 ***Study Area and fieldwork***

169 We sampled mainland populations of the common chaffinch (Fringillidae: *Fringilla coelebs*) and the red-
170 billed chough (Corvidae: *Pyrrhonorax pyrrhonorax*) in the Iberian Peninsula at Segovia and Los Monegros,
171 respectively (see Recuerda et al. 2021, Morinha et al. 2020). The insular populations from both species
172 were sampled in La Palma, the most north-western island of the Canary Islands archipelago (Fig. 1A,

173 Table S1). The common chaffinch lineage in the Canary Islands has recently been raised to species status
174 (Billerman et al. 2022), and we use its current name, Canary Islands chaffinch (*Fringilla canariensis*). The
175 mainland populations of the house finch (Fringillidae: *Haemorhous mexicanus*) and dark-eyed junco
176 (Passerellidae: *Junco hyemalis oreganus*) were sampled in California, and two house finch individuals
177 were sampled in Sierra Juarez (Baja California, Mexico). Insular populations for both species were
178 sampled in Guadalupe Island, Mexico, in the Pacific Ocean (Fig. 1B, Table S1). The junco on Guadalupe
179 Island, until recently a subspecies of *J. hyemalis*, has been raised to species status, and we use its
180 current name, island junco (*Junco insularis*).

181
182 All individuals were captured in the field using mist nets, and also mesh traps in the case of red-billed
183 choughs. All individuals were marked with uniquely numbered aluminum bands, sexed, aged and
184 measured. A blood sample was obtained by venipuncture of the sub-brachial vein and stored in absolute
185 ethanol at -20°C in the laboratory for DNA extraction. After processing, birds were released unharmed at
186 the site of capture. We determined the sex of choughs by the amplification of the *Chd1* gene following
187 Griffiths et al. (1996).

188

189 ***Morphological data and analysis***

190
191 We compared the morphological traits of adult males from mainland and insular populations for all
192 species using principal components analysis (PCA) of all variables and univariate analysis of variance
193 (ANOVA) to compare the means among treatments for each species. For the common chaffinch, the
194 junco and the house finch a wing ruler was used to measure unflattened wing length to the nearest 0.5
195 mm, and dial callipers of 0.1-mm precision were used to measure tail length, tarsus length, bill culmen,
196 total bill length, bill width and bill depth, following Milá et al. (2008). All measurements were taken by a
197 single observer (BM). For the red billed chough, the same traits were measured by a single observer (GB)
198 following standard methods described previously (Blanco et al., 1996).

199 The PCA including all morphological variables was computed using the *prcomp* function in *stats R*
200 package.

201 ***Genome resequencing***

202 Genomic DNA was extracted with a QIAGEN Blood and Tissue kit following the manufacturer's protocol.
203 Resequencing at 18x coverage of 24 individuals per species (12 per treatment, but only 9 for the

204 mainland common chaffinch) was conducted on a SE50 Illumina™ platform at Novogene™. Reads were
205 trimmed with *Trim Galore* (Krueger, 2015) and mapped to their respective reference genomes using
206 BWA (Burrows-Wheeler Aligner, Li & Durbin, 2009). For the common chaffinch and the house finch we
207 used the common chaffinch reference genome (GCA_015532645.2, Recuerda et al., 2021); for the junco
208 we used the *Junco hyemalis* reference genome (GCA_003829775.1, Friis et al., 2022); and for the red-
209 billed chough we used the *Corvus moneduloides* reference genome (GCA_009650955.1, bCorMon1.pri).
210 SNPs were called using BCFTOOLS v.1.3.1 (Danecek et al., 2021) including invariant sites. Filtering was
211 performed with VCFTOOLS v. 0.1.15 (Danecek et al., 2011) separately for variant and invariant sites,
212 using the following criteria for variant sites: (i) Indels and sites with more than two alleles were
213 removed; (ii) a number of reads per site between 10 and 40; (iii) a minimal genotype quality of 30; (iv) a
214 minor allele frequency of 0.01; and (v) 25% maximum missing data and for invariant sites a minimal
215 genotype quality of 30. Variant and invariant sites were then merged using BCFTOOLS concat. The
216 reference genomes from all four species were aligned to the zebra finch genome (*Taeniopygia guttata*,
217 bTaeGut2.pat.W.v2) using nucmer from the MUMmer package (v.4.0, '-b 400' and filtering with 'delta-
218 filter -1'; Marçais et al., 2018) and chromosomes were numbered accordingly (see Table S2, Fig. S1).
219

220 ***Inference of demographic history***

221 The change in effective population size (N_e) across time for each species was estimated using Pairwise
222 Sequentially Markovian Coalescent (PSMC) analysis (Li & Durbin, 2011). The PSMC model infers
223 demographic history based on genome-wide heterozygous sequence data. We used SAMTOOLS (Li et al.,
224 2009) to obtain diploid consensus sequences from BAM files generated with BWA-mem (Li & Durbin,
225 2009). Sites with sequencing depth lower than 10 and higher than 35 were removed. Because sex
226 chromosomes can show different rates and patterns of evolution than autosomes (reviewed by Irwin,
227 2018; Wright & Mank, 2013), we focused our comparisons of differentiation statistics on autosomes
228 only. We converted the diploid consensus sequence to PSMC input files (psmcfa) using the tool
229 fq2psmcfa included in the PSMC software. Then, the program PSMC was used to infer the population
230 history with the options '-N25 -t5 -r1 -p "4+30*2+4+6+10"', except for the mainland common chaffinch,
231 and for both populations of the house finch, where the upper time limit was set to 1 (-t1) to achieve
232 convergence. We performed 100 bootstraps for one genome per species and treatment. The atomic
233 time interval was set following Nadachowska-Brzyska et al., (2016). We used a mutation rate of 4.6 e-9
234 mutations/site/generation (Smeds et al., 2016), which has been used in other avian systems for PSMC

235 analysis (e.g., Ericson et al., 2017; Hanna et al., 2017; Sato et al., 2020; Campana et al., 2020).
236 Generation time was set to two years for all species (Baker & Marshall, 1999; Reid et al., 2003; Møller,
237 2006; Friis et al., 2016).

238

239 ***Inference of recombination rate***

240 In order to determine the effect of recombination rate on the genomic landscapes of differentiation, we
241 estimated recombination rates across the genome for insular and continental populations for the four
242 species using LDhat software (Mcvean & Auton, 2007). First, we created a modified likelihood lookup
243 table based on the LDhat precomputed tables using a sample size of 12 per treatment (9 for the
244 continental common chaffinch) and a population mutation rate parameter estimate of 0.001. Then vcf
245 files were split into chunks of 10,000 SNPs and converted to ldhat format using VCFTOOLS v. 0.1.15
246 (Danecek et al., 2011). The input files generated were used in LDhat “interval” to estimate the effective
247 recombination rate by implementing a Bayesian MCMC sampling algorithm with five million iterations,
248 sampling every 5,000 steps and a block penalty of 10. Finally, the results were summarized using the
249 LDhat module “stat”, discarding 20% of the samples as burn-in.

250

251 ***Genome scans and detection of selective sweeps***

252 In order to detect genomic signatures of selection among the island and mainland counterparts from the
253 four different species, we estimated two different statistics, the fixation index (F_{ST} , Weir & Cockerham,
254 1984) and the cross-population extended haplotype homozygosity (XP-EHH) (Sabeti et al., 2007). First,
255 F_{ST} , d_{xy} and π using were calculated in non-overlapping windows of 10Kb using pixy v. 2 (Korunes &
256 Samuk, 2021). Pixy takes into account the invariant sites for π and d_{xy} calculations, thus overcoming the
257 problem of most programs that use VCF files to calculate those statistics but do not distinguish among
258 invariant and missing sites, resulting in deflated estimates (Korunes & Samuk, 2021). We also computed
259 Tajima’s D (Tajima, 1989) in non-overlapping 10-Kb windows with VCFTOOLS (Danecek et al., 2011). The
260 averaged values of each variable were then transformed to Z-scores using the “scale” command in R. To
261 detect F_{ST} , outliers we corrected for multiple testing setting the false discovery rate (FDR) to 0.05
262 (Benjamini & Hochberg, 1995).

263

264 To detect selective sweeps, we computed the cross-population extended haplotype homozygosity (XP-
265 EHH, Sabeti et al., 2007) using the R package *rehh* (Gautier et al., 2017). First, we phased the vcf files

266 containing only the variant sites in 50-Kb windows using Shapeit v2.r904 (Delaneau et al., 2013). The XP-
267 EHH is based on the comparison of haplotype lengths between populations and has most detection
268 power when the selected haplotype is near fixation in one population and still polymorphic in the other.
269 The genomic regions showing a $-\log_{10}(\text{p-value}) \geq 3$ were considered to be under selection. Then, we
270 looked for overlapping regions between the F_{ST} and the XP-EHH outliers. We generated Manhattan plots
271 for all the statistics using the R package *qqman* (Turner, 2018) in R v. 3.6 (R Core Team, 2018).

273 ***Detecting putative chromosomal inversions***

274 In order to detect potential chromosomal inversions, we examined how patterns of population structure
275 varied along the genome using the R package *lostruct* (Li & Ralph, 2019). SNP data for each species
276 including only variant sites was converted to BCF format using BCFTOOLS version 1.9 (Li et al., 2009). We
277 implemented the script provided by Huang et al. (2020), dividing the genome into 1,000-SNP non-
278 overlapping windows and applying a principal components analysis (PCA) to each window. Euclidian
279 distances between the two first principal components (PCs) between windows were calculated and
280 mapped using multidimensional scaling (MDS) into a 40-dimensional space in order to see the similarity
281 of the relatedness patterns between windows. To identify genomic regions with extreme MDS values,
282 windows with absolute values greater than 4 SD over the mean across all windows were selected for
283 each MDS coordinate. We performed 1,000 permutations of windows over chromosomes to test if
284 outlier regions were randomly distributed across chromosomes. The putative inversion coordinates
285 were the start position of the first outlier window and the end position of the last outlier window. The
286 script included additional analyses to check if the MDS outliers were detecting inversions or instead
287 other processes such as linked selection. First, a PCA was performed using the SNPs from each putative
288 inversion with *SNPRelate* (Zheng et al., 2012). Inversions in the PCA would split the samples into three
289 different groups (i.e., the two orientations and the heterozygotes in an intermediate cluster). The R
290 function *kmeans* with the Hartigan & Wong (1979) method was used to identify the composition of
291 groups of genotypes by performing clustering on the first PC, setting the initial cluster centers as the
292 maximum, minimum and middle of the PC score range. Then, another test was performed averaging the
293 individual heterozygosity per group detected by the k-means clustering. Inversions would show a
294 pattern of higher heterozygosity of the central group relative to the other two groups. Finally, only MDS
295 outlier regions that clustered into three groups in the PCA and showed higher heterozygosity in the
296 middle group were considered as putative inversions.

297

298 ***Candidate genes and GO-term enrichment analysis***

299 We extracted the candidate genes of the genomic regions detected to be under selection by both
300 methods separately (F_{ST} and XP-EHH outliers) using bedtools intersect and the annotation of their
301 respective reference genomes. We checked their functions in *genecards* (Rappaport et al., 2017). We
302 obtained the GO terms using the zebra finch dataset in *biomaRt* in R. We then performed a Gene
303 ontology (GO) enrichment analysis for each set of outliers in the category “biological function” using the
304 *TopGO* R package (Alexa & Rahnenfuhrer, 2016). To estimate the statistical significance, we used the
305 Fisher exact test implementing the *weight01* method. As recommended by the *TopGO* authors, we did
306 not implement corrections for multiple testing and presented raw p-values for the top-10 GO terms
307 related to biological processes.

308

309 **Results**

310 ***Morphological differences***

311 The morphological analysis revealed marked differences in most traits between insular and continental
312 populations for all species. The small species (common chaffinch, junco and house finch), shared a
313 pattern of significantly larger values for most traits in the insular populations compared to mainland,
314 except for the junco wing length, which was longer in the continent (Table S3). In the larger sized red-
315 billed chough, we detected the opposite pattern, with significantly smaller values for most
316 morphological traits in the insular populations, except for bill width, which was smaller in the continent
317 (Table S3). The PC1 for all species showed significant differences among insular and mainland
318 populations, explaining over 39% of the variance in all cases (Fig. 2).

319

320 ***Whole-genome resequencing***

321 The total number of sites obtained in the variant calling was close to the length of the reference
322 genomes. The number of variant sites (40-50 million) was similar for all species except for the red-billed
323 chough, which was lower (~13 million), and the same pattern was maintained after filtering (Table S4).
324 The lower number of variants of the red-billed chough is consistent with its recent divergence, although

325 the house finch shows a high level of polymorphism, comparable to the other two species that diverged
326 a longer time ago.

327 *Inference of demographic history*

328 PSMC-based demographic inference revealed a consistent pattern for the four species, showing stable
329 or growing effective population sizes for mainland populations and a sharp reduction in effective
330 population size in insular populations following colonization. The island-mainland divergence time
331 estimates obtained from the PSMC analysis are around 900,000 years for the common chaffinch,
332 100,000 years for the house finch, 400,000 years for the dark-eye junco, and 30,000 years for the red-
333 billed chough (Fig. 3, S2). The continental population of the red-billed chough showed the smallest
334 effective population size, and the smallest difference between the continental and insular populations
335 among the study species.

336

337 *Inferring parallel evolution from genome-wide scans*

338 Genome-wide scans of genetic differentiation showed high heterogeneity across the four target species.
339 The F_{ST} genomic landscapes varied strongly among species (Fig. 4-7). Mean F_{ST} was higher in the common
340 chaffinch, followed by the dark-eyed junco, as expected for relatively longer island-mainland divergence
341 times. The red-billed chough showed a slightly higher mean F_{ST} than the house finch (Table 1). The red-
342 billed chough's genetic diversity was one order of magnitude lower than the rest, both for insular and
343 mainland populations. The insular common chaffinch population showed the second lowest genetic
344 diversity while the continental population showed the highest diversity value (Table 1). All species
345 showed consistently higher gene content and recombination rates at microchromosomes, and in
346 general, recombination rates were higher at chromosome extremes (Fig. 4-7).

347

348 The red-billed chough genomic landscape shows high levels of relative differentiation across the whole
349 genome with few outlier regions. Mean genetic diversity in both populations is one order of magnitude
350 lower than in the other three species (Table 1), showing very low values across the entire genome
351 except in the microchromosomes, where genetic diversity and divergence show higher values at regions
352 of high gene content. However, the XP-EHH analysis revealed evidence of selective sweeps, showing a
353 few clear peaks along the genome that coincide with drops in Tajima's D (Fig.4).

354

355 The common chaffinch genome landscape is characterized by several F_{ST} peaks that coincide with valleys
356 in d_{xy} and π , and peaks in Tajima's D mainly in the continent (i.e., peaks in chromosomes 1,1A, 2, 3, 4,
357 4A, 6, Fig. 5). This pattern is consistent with the model of recurrent selection, which states that selection
358 in the ancestor previous to the mainland-island split, generates a pattern of low d_{xy} and subsequent
359 selection after divergence reduces genetic diversity, generating F_{ST} peaks. XP-EHH detected selective
360 sweeps mostly concentrated in the microchromosomes and the Z chromosome; few of them coincided
361 with F_{ST} peaks.

362

363 The dark-eyed junco genomic landscape is highly differentiated across the entire genome, and there are
364 few outlier genomic regions, which often coincide with chromosomal extremes (Fig. 6). The XP-EHH
365 scans did not detect significant selective sweeps across the genome, with only three small regions
366 detected.

367

368 The house finch genomic landscape is characterized by a large, highly differentiated region in the middle
369 of chromosome 3, representing 47 million base pairs, suggesting a large chromosomal inversion. It
370 coincides with high values of Tajima's D in the continental population and a region of low
371 recombination, while d_{xy} and π show regular values (Fig. 7). At the end of the same chromosome and at
372 the beginning of chromosome 4, there are two F_{ST} peaks that coincide with a valley in d_{xy} and π , and a
373 peak in Tajima's D. This pattern is consistent with the recurrent selection model. The
374 microchromosomes show high relative differentiation along with high recombination rates and enriched
375 gene content. The XP-EHH scan showed a relatively flat landscape with no evidence for significant
376 selective sweeps.

377

378 ***Detecting putative chromosomal inversions***

379 After combining all possible evidence, the analysis to detect inversions revealed that the red-billed
380 cough genome has no putative inversions. The dark-eyed junco genome showed two possible inverted
381 regions in chromosomes 6 and 7 (Table S5, Fig. S3A) but neither of them coincided with an F_{ST} outlier
382 region. The common chaffinch genome showed two possible inversions in chromosomes 2 and 4, and
383 both coincided with F_{ST} outlier regions (Table S5, Fig. S3B). The house finch genome revealed five
384 putative inversions, a large one in chromosome 3, one in chromosome 1A, and three in chromosome 1.
385 (Table S5, Fig. S3C). Only the large inversion in chromosome 3 coincides with an F_{ST} outlier region (Fig. 7).

386

387 ***Detection of candidate genes and GO-term enrichment analysis***

388 Sharing of candidate genes among species was limited. There were only two genes putatively under
389 selection that were shared between two species: the *morc2* gene was shared between the house finch
390 and the dark-eyed junco, and the *spef2* gene was shared between the dark-eyed junco and the common
391 chaffinch. The *morc2* gene is associated with Marie-Tooth Disease, Axonal, Type 2z (CMT2Z) and
392 Developmental Delay, Impaired Growth, Dysmorphic Facies, and Axonal Neuropathy (DIGFAN) diseases
393 in humans. CMT2Z is characterized by distal lower limb muscle weakness and sensory impairment
394 (Vujovic et al., 2021) and DIGFAN by impaired motor and intellectual development, poor overall growth,
395 usually short body height and microcephaly and subtly dysmorphic facial features in humans (Sacoto et
396 al., 2020). The *spef2* gene is involved in sperm development and also plays a role in osteoblast
397 differentiation, being required for normal bone growth (Lehti et al., 2018).

398

399 In the red-billed chough, the F_{ST} outliers mapped to 19 genes and the XP-EHH outliers detected
400 selective sweeps in 14 genes, without overlap between the two methods. Due to the high relative
401 differentiation across the genome and the absence of clear F_{ST} peaks, the clear selective sweeps along
402 the genome could be a better approach to detect candidates for the red-billed chough. However, most
403 of the genes among the 14 outlier genes found within sweeps have unknown functions, and only five
404 genes have known functions and associated GO terms. From the 20,580 available genes from the *Corvus*
405 *moneduloides* genome, only 8,632 from the gene universe (including the five significant genes) could be
406 used for the analysis. Among the top-10 GO terms for the XP-EHH outliers we found several related to
407 chromatin cohesion (i.e., regulation of cohesion loading and negative regulation of sister chromatid
408 cohesion) (Table S6).

409

410 In the common chaffinch, the genomic scan detected 85 genes in the F_{ST} outlier regions, and the XP-EHH
411 revealed 1,724 outliers that mapped to 21 genes, 3 of which were shared with the F_{ST} candidates. Among
412 the 16,563 genes available in the gene universe, the GO term analysis detected 9,065 feasible genes,
413 including 48 out of the 85 significant genes detected as F_{ST} outliers. Among the top-10 GO terms we
414 found several involved in transcription regulation such as “transcription-dependent tethering of RNA
415 polymerase II gene DNA at nuclear periphery” and “histone H3-K4 acetylation”, and others affecting
416 translation like “lysyl-tRNA aminoacylation” (Table S7). There were also two terms related to cell

417 adhesion “regulation of protein localization to cell-cell adherens junction” and “regulation of focal
418 adhesion assembly”, as well as two terms associated with the organization of cellular components
419 including: “positive regulation of endosome organization” and “lysosome localization”.

420

421 In the dark-eyed junco, the F_{ST} genome scan detected relatively few peaks distributed across the genome
422 that mapped to 24 genes, and three regions were detected as sweeps by the XP-EHH scan but did not
423 contain known genes. Among the 24 genes, only 16 had GO terms associated with them. The GO
424 enrichment analysis performed with a gene universe of 17,038 genes found 9,220 feasible genes
425 including 15 potential candidate genes. The top-10 GO terms revealed three terms related to the
426 centrosome, including “negative regulation of protein localization to centrosome”, “protein localization
427 to pericentriolar material” and “positive regulation of mitotic centrosome separation” (Table S8).

428

429 Finally, in the house finch, the F_{ST} genome scan detected 111 genes putatively under selection, while the
430 XP-EHH scan detected no significant outliers. From the genes identified under selection, 20 were
431 clustered in the middle region of chromosome 3, and two were at the end of the same chromosome.
432 The remaining genes were mainly clustered within microchromosomes. From the 16,563 available genes
433 in the gene universe, 9,065 including 83 significant genes could be used in the GO enrichment analysis.
434 Within the top-10 significant GO terms (Table S9) we find “growth plate cartilage chondrocyte
435 morphogenesis” which is involved in skeletal development and morphogenesis. Also involved in
436 morphogenesis we found the term “zonula adherens maintenance” which is related to cell-cell
437 adhesion. We also find several terms associated with transcription, including “negative regulation of
438 telomerase RNA reverse transcriptase activity”, “glutamyl-tRNA aminoacylation” and two histone
439 acetylations (H2-K14 and H3-K23).

440

441 **Discussion**

442 Our comparative analysis of mainland and insular populations of four passerine species yielded shared
443 patterns of phenotypic divergence and demographic history, in contrast to species-specific patterns of
444 related genome-wide variation. Relative to the mainland, all insular populations showed changes in
445 body size, and suffered reductions in effective population size and genetic diversity, patterns that are
446 consistent with previous findings (Frankham, 1997; Leroy et al., 2021; Benitez et al., 2021). Island
447 colonizations are usually initiated by a small group of individuals, and the resulting genetic drift,
448 combined with the small size of the island’s geographic area, leads to a small effective population size

449 and low genetic diversity (Leroy et al., 2021; Frankham, 1995). Among the four species, the red-billed
450 chough showed the smallest effective population size in both insular and mainland populations, which
451 corresponds to the lowest levels of genetic diversity. In the mainland, this species has shown marked
452 levels of genetic structure in the absence of geographic barriers, suggesting that social barriers due to
453 complex behavioral interactions may constrain gene flow and thus the effective size of local populations
454 (Morinha et al., 2017); the insular population is unlikely to be an exception (Morinha et al., 2020).

455

456 Using PC1 and mean differences in tarsus length, as proxies for structural body size in birds (Jolicoeur,
457 1963; Rising & Somers, 1989; Freeman & Jackson, 1990; Senar & Pascual, 1997), we found that the three
458 smaller passerines increased in size and the larger species suffered a size reduction upon island
459 colonization. This is consistent with the island rule, which posits that small birds evolve towards a larger
460 size and large birds towards a smaller size upon island colonization (Clegg & Owens, 2002; Benitez et al.,
461 2021). However, the difference in the house finch tarsus length among insular and mainland populations
462 was not significant probably due to the small sample size. Regarding beak size, we find that insular
463 individuals from the small sized and short-billed species show longer bills than their mainland
464 counterparts whereas the insular population of the long-billed chough species shows a reduction in bill
465 length. All the species show also differences in at least other bill dimension; however, the red billed
466 chough is the only one in which the change is in the opposite direction, showing shorter but wider bills
467 on the island. The beak is both a feeding and thermoregulatory structure with great evolutionary
468 potential that allows birds to quickly adapt to new environmental conditions (Grant & Grant, 2011) and
469 therefore plays a fundamental role in avian fitness (Grant, 1999; Boag & Grant, 1981; Price et al., 1984;
470 Gibbs & Grant, 1987; Tattersall et al., 2017; Gamboa et al., 2022).

471

472 A major question in evolutionary biology is whether shared phenotypic traits are the result of
473 evolutionary convergence, and the degree to which traits under similar selective pressures share a
474 common genetic basis (Morris, 2010; Blount et al., 2018). Finding shared patterns of genomic variation
475 and common regions of divergence at the intra- or inter-specific levels has been of major interest to
476 understand the mechanisms underlying local adaptation (Burri et al., 2015; Van Doren et al., 2017;
477 Delmore et al., 2018). These shared divergent regions across taxa are particularly interesting when
478 differentiation evolved independently in unrelated lineages (Seehausen et al., 2014). A striking result of
479 our comparative analysis of island-mainland populations in four passerine species is the lack of
480 parallelism in their respective genomic landscapes. We found highly differentiated genomic regions in all

481 four species that were often associated with reduced genetic diversity, suggesting the role of selection
482 in island-mainland differentiation. Yet the lack of congruence in the location of these regions along the
483 genome indicates that the four species adapted to insular environments in different ways, through
484 genetic changes at different loci. Moreover, patterns of recombination rate in these regions suggest that
485 the genomic mechanisms generating these patterns, which include selective sweeps caused by
486 directional selection, chromosomal inversions, and historical factors like recurrent selection, differ in
487 each of the four species.

488

489 According to our demographic analysis, the divergence between red-billed choughs on La Palma and the
490 Iberian Peninsula took place around 30,000 years ago, considering a generation time of two years. A
491 previous study (Morinha et al., 2020) estimated the divergence event in a similar time range, within the
492 last 10,000 years using mitochondrial data and around 30,000 years using iMA2, however they used a
493 generation time of 6 years based on mainland data. If we apply that value, the divergence time estimate
494 changes to around 110,000 years. The red-billed chough also shows the smallest effective population
495 size lowest genetic diversity. This reduced genetic diversity also results in an inflation of the relative
496 divergence (Charlesworth, 1998; Cruickshank & Hahn, 2014), causing a high baseline to detect outliers
497 while the absolute divergence remains low. The recent divergence of the red-billed chough is apparent
498 due to the low divergence along the genome with a mean d_{xy} value of $8.2 \cdot 10^{-4}$. The regions of higher
499 divergence and genetic diversity are located in the microchromosomes, which have relatively higher
500 recombination rates and higher gene content (Burt, 2002). However, the scan for selective sweeps,
501 which is more efficient in detecting recent divergence, revealed clear peaks along the genome. The red-
502 billed chough is the species showing the strongest selective sweeps, which is also consistent with the
503 low genetic diversity of the species due to genomic hitchhiking of the sites flanking selected loci (Kaplan
504 et al., 1989). Among the top ten GO terms of the genes within the selective sweeps there were several
505 related with chromatin cohesion. Specifically, the WAPL gene negatively regulates the association of
506 cohesin with chromatin, having an opposing function to the NIPBL gene. Mutations in the NIPBL gene
507 cause Cornelia de Lange syndrome (CdLS), therefore, mutations in WAPL gene could generate similar
508 developmental deficits to CdLS (Dorsett & Krantz, 2009). CdLS can affect most organ systems, but typical
509 characters include craniofacial structures, upper extremities, eyes and the gastrointestinal system
510 (Jackson et al., 1993; Bhuiyan et al., 2006). The actual role of WAPL has not been properly tested, but it
511 has been associated with Warsaw Breakage Syndrome (WABS) (Faramarz et al., 2019), which is a
512 cohesinopathy that causes growth retardation, severe microcephaly, sensorineural hearing loss,

513 cochlear anomalies, intellectual disability and abnormal skin pigmentation (Alkhunaizi et al., 2018;
514 Faramarz et al., 2019).

515
516 The common chaffinch of La Palma was found to have diverged from its mainland relatives around 0.8-
517 0.9 my ago, which is in agreement with previous reconstructions of the species evolutionary history
518 (Recuerda et al. 2021). A study of the entire common chaffinch radiation across the Atlantic archipelagos
519 revealed that it first colonized Azores, then Madeira and finally the Canary Islands (Recuerda et al.,
520 2021). This sequential colonization of isolated archipelagos has left a genomic signature of recurrent
521 selection along the genome, leading to regions with low absolute divergence due to selection in the
522 ancestor, that were subsequently selected in the daughter populations, reducing genetic diversity and
523 generating F_{ST} peaks (Irwin et al., 2016). This recurrent-selection model fits well with the known
524 colonization history, as the first selective episode probably occurred upon colonization of the Azores,
525 and then at every subsequent colonization step between islands, where successive selective events at
526 the same genomic regions likely led to a loss of genetic diversity. Among the genes associated with
527 outlier loci there were several involved in metabolism (i.e., *fabp2*, *kars1*, *lipa*, *nfrkb*, *pdha1*), five
528 involved in pigmentation and six related to singing. Among the genes related to pigmentation, there
529 were several related to avian plumage coloration, *ap3b1* (Ren et al., 2021), *hps6* (Domyan et al., 2019)
530 and *ric1* (Bruders et al., 2020), one was related to sexual dichromatism in birds (Gazda, 2019), and the
531 *atrn* gene was related to melanin production and has also been associated with coat coloration in
532 macaques (Bradley et al., 2013). Regarding the genes related to song, we detected, *chrm2* and *chrm5*,
533 which have shown differential expression associated with song learning and production in zebra finch
534 (Osogwa, 2018), the *mrps27* (Qi et al., 2012) and *upf3b* (Shi et al., 2021), which are involved in the song
535 control system in the zebra finch, the *paip1* gene, which has been associated with song learning (Lovell
536 et al., 2008), and the *ube2d3* gene, which was related to musical abilities using a convergent evidence
537 method including data from humans, songbirds and other animals (Oikkonen et al., 2016). Interestingly,
538 within the top-ten significant GO terms we detected “positive regulation of endosome organization” and
539 endosomes play an important role in neural development (Yap & Winckler, 2012). We also find the term
540 “regulation of focal adhesion assembly” and it has been shown that cell adhesion plays an important
541 role in tissue morphogenesis (Harris & Tepass, 2010).

542
543 In the dark-eyed junco, the demographic inference revealed that the insular population on Guadalupe
544 diverged around 400,000 years ago, which is similar to previous estimates (Aleixandre et al., 2013). The

545 differentiated regions were mainly distributed at the ends of chromosomes, coinciding with telocentric
546 centromeres, as previously found in Swainson's thrushes (Delmore et al., 2015). Consistent with this
547 pattern, among the top-ten GO terms we identified several that were related to the centrosomes,
548 increasingly recognized as signaling machines capable of regulating many cellular functions (Doxsey et
549 al., 2005).

550

551 In the house finch, the genomic landscape showed signatures of different processes. Despite the recent
552 divergence time between mainland and Guadalupe Island populations, estimated at about 100,000
553 years before present, we did not detect signatures of significant selective sweeps. The large region
554 showing high differentiation and very low recombination in chromosome 3 likely represents a major
555 chromosomal inversion. Genomic islands of differentiation could be generated by chromosomal
556 rearrangements that cluster highly differentiated loci together due to genomic hitchhiking (Yeaman,
557 2013; Huang et al., 2020). However, that could represent either a group of adaptive alleles or several
558 neutral loci linked to a focal selected allele (Yeaman, 2013). Several studies have found regions highly
559 diverged within chromosomal inversions (Hoffmann et al., 2004; Ayala et al., 2014; Christmas et al.,
560 2019; Huang et al., 2020). In this case, 20 genes putatively under selection were found within the
561 inversion. Two of those genes (*fam162b* and *fig4*) are related to facial morphology and related
562 disorders. Little is known about the function of the *fam162b* gene, but it is expressed in mouse facial
563 prominences (Feng et al., 2009), and *fig4* is associated with the Yunis-Varon syndrome, characterized by
564 skeletal defects including cleidocranial dysplasia, digital anomalies and neurological impairment
565 (Campeau et al., 2013). Another interesting candidate is the *lyd* gene, which is also found within an
566 inversion in chromosome 2 in the white-throated sparrow (*Zonotrichia albicollis*) and has shown
567 differences in expression between two morphs that differed in territorial aggression including song
568 (Zinzow-Kramer et al., 2015). Within that inversion, they found mainly genes related to behavior and
569 plumage color. Some genes within the inversion in the house finch are related to mental retardation in
570 humans including FMN2 (Law et al., 2014; Gorukmez et al., 2020), or to behavior in mice, like *pnisr*
571 (Moloney et al., 2019). Interestingly, within the house finch inversion we also found the gene *gtf3c6*,
572 which was found to be a candidate involved in sexual selection in a comparison of 11 bird genomes
573 (Jaiswal et al., 2021). Within the top-ten significant GO terms, we found "growth plate cartilage
574 chondrocyte morphogenesis", which is involved in skeletal development and morphogenesis and
575 regulated by multiple signaling pathways including, among others, the bone morphogenetic proteins
576 (Bmp; De Luca et al., 2001), fibroblast growth factors (FGFs; Deng et al., 1996) and Wingless/int.1

577 molecules (Wnt; Yang et al., 2003). Among these pathways, the Bmp and Wnt signaling pathways are
578 known to be involved in facial development in different organisms including beak morphology in birds
579 (Abzhanov, 2004; Brugmann et al., 2010). We also found the term “zonula adherens maintenance” and
580 it has been shown that the adherens junctions are also involved in tissue morphogenesis (Harris &
581 Tepass, 2010).

582

583 Here we studied four cases of island-mainland divergence in passerine species that have colonized
584 oceanic islands and share phenotypic modifications likely caused by similar selective pressures, and
585 asked whether the underlying genetic mechanisms were also shared. Our general result in this respect is
586 that the regions of the genome showing evidence of divergence under directional selection are lineage
587 specific, suggesting that the genetic basis of phenotypic divergence is different in each case, so that
588 evidence for convergence at the genomic level appears to be lacking (Van Doren et al., 2017). Even if the
589 same regions had been detected as putatively under selection or with shared genomic features involved
590 in genomic differentiation, such as the stable recombination landscape in avian lineages (Singhal et al.,
591 2015), it would be difficult to determine whether that pattern is generated by directional selection or by
592 background and linked selection. Despite examples showing that few loci of large effect can drive
593 adaptive divergence in complex traits, such as the bill (e.g., Enbody et al., 2023), selection is likely to act
594 on many loci of small effect due to the polygenic nature of most adaptive traits (Pritchard & Di Rienzo,
595 2010; Bosse et al., 2017). Consequently, convergent phenotypes could in fact be due to divergent
596 genotypes. Several examples to date show that phenotypic change in a given trait can be driven by
597 different sets of genes, such as mouth morphology in cichlid fishes (Elmer et al., 2014), or color pattern
598 in mice (Hoekstra et al., 2006; Steiner et al., 2009) and flies (Wittkopp et al., 2003). Even though the
599 outlier genes differ among species, there could be common significant GO terms because different
600 genes share functions and pathways. Interestingly, between the common chaffinch and the house finch
601 we found several similar GO terms related to tRNA aminoacylation, histone acetylations and cell
602 adherens junctions. Remarkably, we found that in all four species, GO terms are mostly related to gene
603 regulation, for instance by modifying histones or altering chromatin binding and chromosome
604 condensation, which are essential for differentiation and development. Recently, Monroe et al. (2021)
605 reported that mutations occur less often in functional regions of the genome, and that epigenomic and
606 physical chromosomal features account for the position of the mutations. In our case, most of the terms
607 related to outlier loci are involved in epigenetic modifications, suggesting that changes in gene
608 regulation, instead of specific core genes, may be the main drivers of divergence. Currently, several

609 models are being developed to understand the role of gene regulation in the evolution of complex traits
610 (Boyle et al., 2017; Liu et al., 2019), implying that regulatory regions are disproportionately targeted by
611 polygenic selection, highlighting the key role of gene regulatory networks in evolution (Fagny &
612 Austerlitz, 2021).

613

614 **Data availability**

615 Resequencing raw data is deposited at NCBI under the SRA data projects PRJNA661201 (for common
616 chaffinch mainland population) with accession numbers SAMN16094451-SAMN16094459 and
617 PRJNAXXXXX with accession numbers SAMNXXXXX-SAMNXXXXX, for the common chaffinch insular
618 population and both populations from the rest of the species, see Table S1 for details) and the datasets,
619 are deposited in Figshare (<https://doi.org/10.6084/m9.figshare.21590673>).

620

621 **Acknowledgements**

622 We are grateful to José Manuel González, Óscar Frías and Félix Medina for invaluable help in the field.
623 This work was supported by grants CGL-2015-66381P and PGC-2018-098897-B-I00 from Spain's Ministry
624 of Science and co-financed by the European Union's Regional Development Fund (ERDF). MR was
625 supported by a doctoral fellowship from Spain's Ministry of Education, Culture, and Sport
626 (FPU16/05724).

627

628 **CRedit authorship contribution statement**

629 MR carried out the molecular lab work, carried out the data curation and analysis, participated in the
630 design of the study, collected field data and drafted the manuscript; GB conceived and designed the
631 study, collected field data and critically revised the manuscript; BM conceived and designed the study,
632 collected field data and critically revised the manuscript. All authors gave final approval for publication
633 and agree to be held accountable for the work performed therein.

634

635 **References**

636 Abzhanov, A. (2004). Bmp4 and Morphological variation of beaks in Darwin's Finches. *Science*,
637 305(5689), 1462–1465. <https://doi.org/10.1126/science.1098095>

638 Aleixandre, P., Hernández Montoya, J., & Milá, B. (2013). Speciation on oceanic islands: rapid adaptive
639 divergence vs. cryptic speciation in a Guadalupe Island songbird (Aves: *Junco*). *PLoS ONE*, 8(5) ,
640 e63242. <https://doi.org/10.1371/journal.pone.0063242>

641 Alexa, A., & Rahnenfuhrer, J. (2016). topGO: Enrichment analysis for Gene Ontology. R package version
642 2.28.0. *Cranio*.

643 Alkhunaizi, E., Shaheen, R., Bharti, S. K., Joseph-George, A. M., Chong, K., Abdel-Salam, G. M., ... &
644 Chitayat, D. (2018). Warsaw breakage syndrome: Further clinical and genetic delineation. *American*
645 *Journal of Medical Genetics Part A*, 176(11), 2404-2418. <https://doi.org/10.1002/ajmg.a.40482>

646 Ayala, D., Ullastres, A., & González, J. (2014). Adaptation through chromosomal inversions in *Anopheles*.
647 *Frontiers in Genetics*, 5, 129. <https://doi.org/10.3389/fgene.2014.00129>

648 Baker, A. J., & Marshall, H. D. (1999). Population divergence in Chaffinches *Fringilla coelebs* assessed
649 with control-region sequences. *Proceedings XXII International Ornithological Congress (NJ Adams*
650 *and RH Slotow, Eds.)*. *BirdLife South Africa, Durban*, 1899–1913.

651 Benítez-López, A., Santini, L., Gallego-Zamorano, J., Milá, B., Walkden, P., Huijbregts, M. A. J., & Tobias, J.
652 A. (2021). The island rule explains consistent patterns of body size evolution in terrestrial
653 vertebrates. *Nature Ecology and Evolution*, 5(6), 768–786. [https://doi.org/10.1038/s41559-021-](https://doi.org/10.1038/s41559-021-01426-y)
654 [01426-y](https://doi.org/10.1038/s41559-021-01426-y)

655 Benjamini, Y., & Hochberg, Y. (1995). Controlling the false discovery rate: a practical and powerful
656 approach to multiple testing. *Journal of the Royal Statistical Society: Series B (Methodological)*,
657 57(1), 289–300. <https://doi.org/10.1111/j.2517-6161.1995.tb02031.x>

658 Bhuiyan, Z. A., Klein, M., Hammond, P., Van Haeringen, A., Mannens, M. M. A. M., Van Berckelaer-
659 Onnes, I., & Hennekam, R. C. M. (2006). Genotype-phenotype correlations of 39 patients with
660 Cornelia de Lange syndrome: The Dutch experience. *Journal of Medical Genetics*, 43(7), 568–575.
661 <https://doi.org/10.1136/jmg.2005.038240>

662 Billerman, S. M., Keeney, B. K., Rodewald P. G., and Schulenberg T. S. (Editors) (2022). *Birds of the*
663 *World*. Cornell Laboratory of Ornithology, Ithaca, NY, USA. <https://birdsoftheworld.org/bow/home>

664 Blanco, G., Tella, J. L., and Torre, I. (1996). Age and sex determination of monomorphic non-breeding
665 choughs: A long-term study. *J. Field. Orn.* 67, 428–433.

666 Blanco, G., Laiolo, P., & Fargallo, J. A. (2014). Linking environmental stress, feeding-shifts and the “island
667 syndrome”: A nutritional challenge hypothesis. *Population Ecology*, 56(1), 203–216.
668 <https://doi.org/10.1007/s10144-013-0404-3>

669 Blondel, J. (2000). *Evolution and ecology of birds on islands: trends and prospects*. *Vie et Milieu/Life &*

670 *Environment*, 205-220.

671 Blount, Z. D., Lenski, R. E., & Losos, J. B. (2018). Contingency and determinism in evolution: Replaying
672 life's tape. *Science*, 362(6415), eaam5979. <https://doi.org/10.1126/science.aam5979>

673 Boag, P. T., & Grant, P. R. (1981). Intense natural selection in a population of Darwin's finches
674 (Geospizinae) in the Galapagos. *Science*, 214(4516), 82–85.
675 <https://doi.org/10.1126/science.214.4516.82>

676 Bosse, M., Spurgin, L. G., Laine, V. N., Cole, E. F., Firth, J. A., Gienapp, P., Gosler, A. G., McMahon, K.,
677 Poissant, J., Verhagen, I., Groenen, M. A. M., Van Oers, K., Sheldon, B. C., Visser, M. E., & Slate, J.
678 (2017). Recent natural selection causes adaptive evolution of an avian polygenic trait. *Science*,
679 358(6361), 365–368. <https://doi.org/10.1126/science.aal3298>

680 Boyle, E. A., Li, Y. I., & Pritchard, J. K. (2017). An expanded view of complex traits: from polygenic to
681 omnigenic. *Cell*, 169(7), 1177–1186. <https://doi.org/10.1016/j.cell.2017.05.038>

682 Bradley, B. J., Gerald, M. S., Widdig, A., & Mundy, N. I. (2013). Coat Color Variation and Pigmentation
683 Gene Expression in Rhesus Macaques (*Macaca mulatta*). *Journal of Mammalian Evolution*, 20(3),
684 263–270. <https://doi.org/10.1007/s10914-012-9212-3>

685 Brown, R. M., Siler, C. D., Oliveros, C. H., Esselstyn, J. A., Diesmos, A. C., Hosner, P. A., Linkem, C. W.,
686 Barley, A. J., Oaks, J. R., Sanguila, M. B., Welton, L. J., Blackburn, D. C., Moyle, R. G., Townsend
687 Peterson, A., & Alcala, A. C. (2013). Evolutionary Processes of Diversification in a Model Island
688 Archipelago. *Annual Review of Ecology, Evolution, and Systematics*, 44(1), 411–435.
689 <https://doi.org/10.1146/annurev-ecolsys-110411-160323>

690 Bruders, R., van Hollebeke, H., Osborne, E. J., Kronenberg, Z., Maclary, E., Yandell, M., & Shapiro, M. D.
691 (2020). A copy number variant is associated with a spectrum of pigmentation patterns in the rock
692 pigeon (*Columba livia*). *PLoS Genetics*, 16(5), 1–25. <https://doi.org/10.1371/journal.pgen.1008274>

693 Brugmann, S. A., Powder, K. E., Young, N. M., Goodnough, L. H., Hahn, S. M., James, A. W., Helms, J. A.,
694 & Lovett, M. (2010). Comparative gene expression analysis of avian embryonic facial structures
695 reveals new candidates for human craniofacial disorders. *Human Molecular Genetics*, 19(5), 920–
696 930. <https://doi.org/10.1093/hmg/ddp559>

697 Burri, R. (2017). Interpreting differentiation landscapes in the light of long-term linked selection.
698 *Evolution Letters*, 1(3), 118–131. <https://doi.org/10.1002/evl3.14>

699 Burri, R., Nater, A., Kawakami, T., Mugal, C. F., Olason, P. I., Smeds, L., Suh, A., Dutoit, L., Bureš, S.,
700 Garamszegi, L. Z., Hogner, S., Moreno, J., Qvarnström, A., Ružić, M., Sæther, S. A., Sætre, G. P.,
701 Török, J., & Ellegren, H. (2015). Linked selection and recombination rate variation drive the

702 evolution of the genomic landscape of differentiation across the speciation continuum of *Ficedula*
703 flycatchers. *Genome Research*, 25(11), 1656-1665. <https://doi.org/10.1101/gr.196485.115>

704 Burt, D. W. (2002). Origin and evolution of avian microchromosomes. *Cytogenetic and Genome*
705 *Research*, 96(1–4), 97–112. <https://doi.org/10.1159/000063018>

706 Campana, M. G., Corvelo, A., Shelton, J., Callicrate, T. E., Bunting, K. L., Riley-Gillis, B., Wos, F., Degrazia,
707 J., Jarvis, E. D., & Fleischer, R. C. (2020). Adaptive Radiation Genomics of Two Ecologically Divergent
708 Hawaiʻian Honeycreepers: The ‘akiapōlā‘au and the Hawaiʻi ‘amakihī. *Journal of Heredity*, 111(1),
709 21–32. <https://doi.org/10.1093/jhered/esz057>

710 Campeau, P. M., Lenk, G. M., Lu, J. T., Bae, Y., Burrage, L., Turnpenny, P., Román Corona-Rivera, J.,
711 Morandi, L., Mora, M., Reutter, H., Vulto-Van Silfhout, A. T., Faivre, L., Haan, E., Gibbs, R. A.,
712 Meisler, M. H., & Lee, B. H. (2013). Yunis-Varón syndrome is caused by mutations in FIG4, encoding
713 a phosphoinositide phosphatase. *American Journal of Human Genetics*, 92(5), 781–791.
714 <https://doi.org/10.1016/j.ajhg.2013.03.020>

715 Carbeck, K., Arcese, P., Lovette, I., Pruett, C., Winker, K., & Walsh, J. (2023). Candidate genes under
716 selection in song sparrows co-vary with climate and body mass in support of Bergmann’s
717 Rule. *Nature Communications*, 14(1), 6974. <https://doi.org/10.1038/s41467-023-42786-2>

718 Charlesworth, B. (1998). Measures of divergence between populations and the effect of forces that
719 reduce variability. *Molecular Biology and Evolution*, 15(5), 538–543.
720 <https://doi.org/10.1093/oxfordjournals.molbev.a025953>

721 Charlesworth, B., Nordborg, M., & Charlesworth, D. (1997). The effects of background and interference
722 selection on patterns of genetic variation in subdivided populations. *Genetics*, 70, 155–174.
723 <https://doi.org/10.1534/genetics.115.178558>

724 Chase, M. A., Ellegren, H., & Mugal, C. F. (2021). Positive selection plays a major role in shaping
725 signatures of differentiation across the genomic landscape of two independent *Ficedula* flycatcher
726 species pairs. *Evolution*, 75(9), 2179-2196. <https://doi.org/10.1111/evo.14234>

727 Christmas, M. J., Wallberg, A., Bunikis, I., Olsson, A., Wallerman, O., & Webster, M. T. (2019).
728 Chromosomal inversions associated with environmental adaptation in honeybees. *Molecular*
729 *Ecology*, 28(6), 1358–1374. <https://doi.org/10.1111/mec.14944>

730 Clegg, S. (2009). Evolutionary changes following island colonization in birds. *The Theory of Island*
731 *Biogeography Revisited*, 293–325. <https://doi.org/10.1515/9781400831920.293>

732 Clegg, S. M., & Owens, P. F. (2002). The ‘island rule’ in birds: medium body size and its ecological
733 explanation. *Proceedings of the Royal Society of London. Series B: Biological Sciences*, 269(1498),

734 1359-1365.

735 Clements, J. F., P. C. Rasmussen, T. S. Schulenberg, M. J. Iliff, T. A. Fredericks, J. A. Gerbracht, D. Lepage,
736 A. Spencer, S. M. Billerman, B. L. Sullivan, and C. L. Wood. 2023. The eBird/Clements checklist of
737 Birds of the World: v2023. Downloaded
738 from <https://www.birds.cornell.edu/clementschecklist/download/>

739 Colosimo, P. F., Hosemann, K. E., Balabhadra, S., Villarreal Jr, G., Dickson, M., Grimwood, J., ... &
740 Kingsley, D. M. (2005). Widespread parallel evolution in sticklebacks by repeated fixation of
741 ectodysplasin alleles. *science*, 307(5717), 1928-1933. <https://doi.org/10.1126/science.1107239>

742 Cruickshank, T. E., & Hahn, M. W. (2014). Reanalysis suggests that genomic islands of speciation are due
743 to reduced diversity, not reduced gene flow. *Molecular Ecology*, 23(13), 3133-3157..
744 <https://doi.org/10.1111/mec.12796>

745 Danecek, P., Auton, A., Abecasis, G., Albers, C. A., Banks, E., DePristo, M. A., Handsaker, R. E., Lunter, G.,
746 Marth, G. T., Sherry, S. T., McVean, G., & Durbin, R. (2011). The variant call format and VCFtools.
747 *Bioinformatics*, 27(15), 2156–2158. <https://doi.org/10.1093/bioinformatics/btr330>

748 Danecek, P., Bonfield, J. K., Liddle, J., Marshall, J., Ohan, V., Pollard, M. O., Whitwham, A., Keane, T.,
749 McCarthy, S. A., Davies, R. M., & Li, H. (2021). Twelve years of SAMtools and BCFtools. *GigaScience*,
750 10(2), 1–4. <https://doi.org/10.1093/gigascience/giab008>

751 De Luca, F., Barnes, K. M., Uyeda, J. A., De-Levi, S., Abad, V., Palese, T., Mericq, V., & Baron, J. (2001).
752 Regulation of growth plate chondrogenesis by bone morphogenetic protein-2. *Endocrinology*,
753 142(1), 430–436. <https://doi.org/10.1210/endo.142.1.7901>

754 Delaneau, O., Zagury, J. F., & Marchini, J. (2013). Improved whole-chromosome phasing for disease and
755 population genetic studies. *Nature Methods*, 10(1), 5–6. <https://doi.org/10.1038/nmeth.2307>

756 Delmore, K. E., Hübner, S., Kane, N. C., Schuster, R., Andrew, R. L., Câmara, F., Guigó, R., & Irwin, D. E.
757 (2015). Genomic analysis of a migratory divide reveals candidate genes for migration and
758 implicates selective sweeps in generating islands of differentiation. *Molecular Ecology*, 24(8),
759 1873–1888. <https://doi.org/10.1111/mec.13150>

760 Delmore, K. E., Lugo Ramos, J. S., Van Doren, B. M., Lundberg, M., Bensch, S., Irwin, D. E., & Liedvogel,
761 M. (2018). Comparative analysis examining patterns of genomic differentiation across multiple
762 episodes of population divergence in birds. *Evolution Letters*, 2(2), 76-87.
763 <https://doi.org/10.1002/evl3.46>

764 Deng, C., Wynshaw-Boris, A., Zhou, F., Kuo, A., & Leder, P. (1996). Fibroblast growth factor receptor 3 is
765 a negative regulator of bone growth. *Cell*, 84(6), 911–921. <https://doi.org/10.1016/S0092->

766 8674(00)81069-7

767 Domyan, E. T., Hardy, J., Wright, T., Frazer, C., Daniels, J., Kirkpatrick, J., Kirkpatrick, J., Wakamatsu, K., &
768 Hill, J. T. (2019). SOX10 regulates multiple genes to direct eumelanin versus pheomelanin
769 production in domestic rock pigeon. *Pigment Cell and Melanoma Research*, 32(5), 634–642.
770 <https://doi.org/10.1111/pcmr.12778>

771 Dorsett, D., & Krantz, I. D. (2009). On the Molecular Etiology of Cornelia de Lange Syndrome Dale. *Annals*
772 *of the New York Academy of Sciences*, 1151(1), 22–37. <https://doi.org/10.1111/j.1749->
773 [6632.2008.03450.x](https://doi.org/10.1111/j.1749-6632.2008.03450.x). On

774 Dutoit, L., Burri, R., Nater, A., Mugal, C. F., & Ellegren, H. (2017). Genomic distribution and estimation of
775 nucleotide diversity in natural populations: perspectives from the collared flycatcher (*Ficedula*
776 *albicollis*) genome. *Molecular Ecology Resources*, 17(4), 586–597. <https://doi.org/10.1111/1755->
777 [0998.12602](https://doi.org/10.1111/1755-0998.12602)

778 Ellegren, H. (2010). Evolutionary stasis: the stable chromosomes of birds. *Trends in Ecology and*
779 *Evolution*, 25(5), 283–291. <https://doi.org/10.1016/j.tree.2009.12.004>

780 Ellegren, H., Smeds, L., Burri, R., Olason, P. I., Backström, N., Kawakami, T., Künstner, A., Mäkinen, H.,
781 Nadachowska-Brzyska, K., Qvarnström, A., Uebbing, S., & Wolf, J. B. W. (2012). The genomic
782 landscape of species divergence in *Ficedula* flycatchers. *Nature*, 491(7426), 756–760.
783 <https://doi.org/10.1038/nature11584>

784 Elmer, K. R., Fan, S., Kusche, H., Luise Spreitzer, M., Kautt, A. F., Franchini, P., & Meyer, A. (2014). Parallel
785 evolution of Nicaraguan crater lake cichlid fishes via non-parallel routes. *Nature Communications*,
786 5(1), 1-8. <https://doi.org/10.1038/ncomms6168>

787 Enbody, E. D., Sendell-Price, A. T., Sprehn, C. G., Rubin, C. J., Visscher, P. M., Grant, B. R., ... & Andersson,
788 L. (2023). Community-wide genome sequencing reveals 30 years of Darwin’s finch
789 evolution. *Science*, 381(6665), eadf6218. <https://doi.org/10.1126/science.adf6218>

790 Ericson, P. G. P., Qu, Y., Blom, M. P. K., Johansson, U. S., & Irestedt, M. (2017). A genomic perspective of
791 the pink-headed duck *Rhodonessa caryophyllacea* suggests a long history of low effective
792 population size. *Scientific Reports*, 7(1), 1–6. <https://doi.org/10.1038/s41598-017-16975-1>

793 Fagny, M., & Austerlitz, F. (2021). Polygenic Adaptation: Integrating Population Genetics and Gene
794 Regulatory Networks. *Trends in Genetics*, 37(7), 631–638.
795 <https://doi.org/10.1016/j.tig.2021.03.005>

796 Faramarz, A., Balk, J. A., Oostra, A. B., Ghandour, C. A., Roomans, M. A., Wolthuis, R. M. F., & de Lange,
797 J. (2019). Non-redundant roles in sister chromatid cohesion of the DNA helicase DDX11 and the

798 SMC3 acetyl transferases ESCO1/2. *BioRxiv*, 1–19. <https://doi.org/10.1101/704635>

799 Feder, J. L., & Nosil, P. (2010). The efficacy of divergence hitchhiking in generating genomic islands
800 during ecological speciation. *Evolution*, 64(6), 1729–1747. [https://doi.org/10.1111/j.1558-](https://doi.org/10.1111/j.1558-5646.2009.00943.x)
801 5646.2009.00943.x

802 Feng, W., Leach, S. M., Tipney, H., Phang, T., Geraci, M., Spritz, R. A., Hunter, L. E., & Williams, T. (2009).
803 Spatial and temporal analysis of gene expression during growth and fusion of the mouse facial
804 prominences. *PLoS ONE*, 4(12), e8066. <https://doi.org/10.1371/journal.pone.0008066>

805 Feng, S., Stiller, J., Deng, Y., Armstrong, J., Fang, Q. I., Reeve, A. H., ... & Zhang, G. (2020). Dense sampling
806 of bird diversity increases power of comparative genomics. *Nature*, 587(7833), 252-
807 25. <https://doi.org/10.1038/s41586-020-2873-9>

808 Ferchaud, A. L., & Hansen, M. M. (2016). The impact of selection, gene flow and demographic history on
809 heterogeneous genomic divergence: Three-spine sticklebacks in divergent environments.
810 *Molecular Ecology*, 25(1), 238–259. <https://doi.org/10.1111/mec.13399>

811 Foster, J. B. (1964). Evolution of mammals on islands. *Nature*, 202(4929), 234-235.

812 Frankham, R. (1995). Effective population size/adult population size ratios in wildlife: A review. *Genetics*
813 *Research*, 89(5–6), 491–503. <https://doi.org/10.1017/S0016672308009695>

814 Frankham, R. (1997). Do island populations have less genetic variation than mainland populations?
815 *Heredity*, 78(3), 311–327. <https://doi.org/10.1038/hdy.1997.46>

816 Freeman, S., & Jackson, W. M. (1990). Univariate metrics are not adequate to measure avian body
817 size. *The Auk*, 107(1), 69-74.

818 Friis, G., Aleixandre, P., Rodríguez-Estrella, R., Navarro-Sigüenza, A. G., & Milá, B. (2016). Rapid
819 postglacial diversification and long-term stasis within the songbird genus *Junco*: phylogeographic
820 and phylogenomic evidence. *Molecular Ecology*, 25(24), 6175–6195.
821 <https://doi.org/10.1111/mec.13911>

822 Gamboa, M. P., Ghalambor, C. K., Scott Sillett, T., Morrison, S. A., & Chris Funk, W. (2022). Adaptive
823 divergence in bill morphology and other thermoregulatory traits is facilitated by restricted gene
824 flow in song sparrows on the California Channel Islands. *Molecular Ecology*, 31(2), 603–619.
825 <https://doi.org/10.1111/mec.16253>

826 Gautier, M., Klassmann, A., & Vitalis, R. (2017). rehh 2.0: a reimplementation of the R package rehh to
827 detect positive selection from haplotype structure. *Molecular Ecology Resources*, 17(1), 78–90.
828 <https://doi.org/10.1111/1755-0998.12634>

829 Gazda, M. A. (2019). Genetic basis of simple and complex traits with relevance to avian evolution.

830 Gibbs, H. L., & Grant, P. R. (1987). Oscillating selection on Darwin's finches. *Nature*, 327(6122), 511–513.
831 <https://doi.org/10.1038/327511a0>

832 Gillespie, R. G., Bennett, G. M., De Meester, L., Feder, J. L., Fleischer, R. C., Harmon, L. J., ... & Wogan, G.
833 O. (2020). Comparing adaptive radiations across space, time, and taxa. *Journal of Heredity*, 111(1),
834 1-20. <https://doi.org/10.1093/jhered/esz064>

835 Glor, R. E., Gifford, M. E., Larson, A., Losos, J. B., Rodríguez Schettino, L., Chamizo Lara, A. R., & Jackman,
836 T. R. (2004). Partial island submergence and speciation in an adaptive radiation: A multilocus
837 analysis of the Cuban green anoles. *Proceedings of the Royal Society B: Biological Sciences*,
838 271(1554), 2257–2265. <https://doi.org/10.1098/rspb.2004.2819>

839 Gorukmez, O., Gorukmez, O., & Ekici, A. (2020). A novel nonsense FMN2 mutation in Nonsyndromic
840 Autosomal Recessive Intellectual Disability Syndrome. *Fetal and Pediatric Pathology*, 40(6), 702-
841 706. <https://doi.org/10.1080/15513815.2020.1737991>

842 Grant, P. R. (1999). *Ecology and evolution of Darwin's finches*. Princeton University Press.

843 Grant, P. R. (2001). Reconstructing the evolution of birds on islands: 100 years of research. *Oikos*, 92(3),
844 385–403. <https://doi.org/10.1034/j.1600-0706.2001.920301.x>

845 Grant, P. R., & Grant, B. R. (2002). Adaptive Radiation of Darwin's Finches. *American Scientist*, 90(2),
846 130–139. <https://doi.org/10.1511/2002.2.130>

847 Grant, P. R., & Grant, B. R. (2011). *How and why species multiply: the radiation of Darwin's finches*.
848 Princeton University Press.

849 Griffiths, R., Daan, S., & Dijkstra, C. (1996). Sex identification in birds using two CHD genes. *Proceedings*
850 *of the Royal Society of London. Series B: Biological Sciences*, 263(1374), 1251-1256.

851 Sacoto, M. J. G., Tchasovnikarova, I. A., Torti, E., Forster, C., Andrew, E. H., Anselm, I., ... & Juusola, J.
852 (2020). De novo variants in the ATPase module of MORC2 cause a neurodevelopmental disorder
853 with growth retardation and variable craniofacial dysmorphism. *The American Journal of Human*
854 *Genetics*, 107(2), 352-363. <https://doi.org/10.1016/j.ajhg.2020.06.013>

855 Han, F., Lamichhaney, S., Rosemary Grant, B., Grant, P. R., Andersson, L., & Webster, M. T. (2017). Gene
856 flow, ancient polymorphism, and ecological adaptation shape the genomic landscape of divergence
857 among Darwin's finches. *Genome Research*, 27(6), 1004-1015.
858 <https://doi.org/10.1101/gr.212522.116>

859 Hanna, Z. R., Henderson, J. B., Wall, J. D., Emerling, C. A., Fuchs, J., Runckel, C., Mindell, D. P., Bowie, R.
860 C. K., DeRisi, J. L., & Dumbacher, J. P. (2017). Northern spotted owl (*Strix occidentalis caurina*)
861 genome: Divergence with the barred owl (*Strix varia*) and characterization of light-associated

862 genes. *Genome Biology and Evolution*, 9(10), 2522–2545. <https://doi.org/10.1093/gbe/evx158>

863 Harris, T. J. C., & Tepass, U. (2010). Adherens junctions: from molecules to morphogenesis. *Nature*

864 *Reviews Molecular Cell Biology*, 11(7), 502–514. <https://doi.org/10.1038/nrm2927>

865 Hartigan, J. A., & Wong, M. A. (1979). Algorithm AS 136: A k-means clustering algorithm. *Journal of the*

866 *Royal Statistical Society. Series C (Applied Statistics)*, 28(1), 100-108.

867 <https://doi.org/10.2307/2346830>

868 Hoekstra, H. E., Hirschmann, R. J., Bunday, R. A., Insel, P. A., & Crossland, J. P. (2006). A Single Amino

869 Acid Mutation Contributes to Adaptive Beach Mouse Color Pattern. *Science*, 313(5783), 101–104. .

870 <https://doi.org/10.1126/science.1126121>

871 Hoffmann, A. A., Sgrò, C. M., & Weeks, A. R. (2004). Chromosomal inversion polymorphisms and

872 adaptation. *Trends in Ecology and Evolution*, 19(9), 482–488.

873 <https://doi.org/10.1016/j.tree.2004.06.013>

874 Huang, K., Andrew, R. L., Owens, G. L., Ostevik, K. L., & Rieseberg, L. H. (2020). Multiple chromosomal

875 inversions contribute to adaptive divergence of a dune sunflower ecotype. *Molecular Ecology*,

876 29(14), 2535–2549. <https://doi.org/10.1111/mec.15428>

877 Irwin, D. E., Alcaide, M., Delmore, K. E., Irwin, J. H., & Owens, G. L. (2016). Recurrent selection explains

878 parallel evolution of genomic regions of high relative but low absolute differentiation in a ring

879 species. *Molecular Ecology*, 25(18), 4488–4507. <https://doi.org/10.1111/mec.13792>

880 Irwin, D. E., Milá, B., Toews, D. P. L., Brelsford, A., Kenyon, H. L., Porter, A. N., Grossen, C., Delmore, K. E.,

881 Alcaide, M., & Irwin, J. H. (2018). A comparison of genomic islands of differentiation across three

882 young avian species pairs. *Molecular Ecology*, 27(23), 4839-4855.

883 <https://doi.org/10.1111/mec.14858>

884 Jackson, L., Kline, A. D., Barr, M. A., & Koch, S. De. (1993). de Lange syndrome: a clinical review of 310

885 individuals. *American Journal of Medical Genetics*, 47(7), 940–946.

886 <https://doi.org/10.1002/ajmg.1320470703>

887 Jaiswal, S. K., Gupta, A., Shafer, A. B. A., Vishnu Prasoodanan, P. K., Vijay, N., & Sharma, V. K. (2021).

888 Genomic insights into the molecular basis of sexual selection in birds. *Frontiers in Ecology and*

889 *Evolution*, 9:538498. <https://doi.org/10.3389/fevo.2021.538498>

890 Jolicoeur P. (1963). The multivariate generalization of the allometry equation. *Biometrics* 19: 497-499.

891 Kaplan, N. L., Hudson, R. R., & Langley, C. H. (1989). The " hitchhiking effect" revisited. *Genetics*, 123(4),

892 887-899. <https://doi.org/10.1093/genetics/123.4.887>

893 Kawakami, T., Mugal, C. F., Suh, A., Nater, A., Burri, R., Smeds, L., & Ellegren, H. (2017). Whole-genome

894 patterns of linkage disequilibrium across flycatcher populations clarify the causes and
895 consequences of fine-scale recombination rate variation in birds. *Molecular Ecology*, 26(16), 4158–
896 4172. <https://doi.org/10.1111/mec.14197>

897 Korunes, K. L., & Samuk, K. (2021). pixy: Unbiased estimation of nucleotide diversity and divergence in
898 the presence of missing data. *Molecular Ecology Resources*, 21(4), 1359–1368.
899 <https://doi.org/10.1111/1755-0998.13326>

900 Krueger, F. (2015). Trim galore. *A wrapper tool around Cutadapt and FastQC to consistently apply quality*
901 *and adapter trimming to FastQ files*, 516(517).

902 Krzywinski, M., Schein, J., Gascoyne, R., Connors, J., Horsman, D., Jones, S. J., & Marra, M. A. (2009).
903 Circos : An information aesthetic for comparative genomics. *Genome Research*, 19(604), 1639–
904 1645. <https://doi.org/10.1101/gr.092759.109.19>

905 Lapiedra, O., Sayol, F., Garcia-Porta, J., & Sol, D. (2021). Niche shifts after island colonization spurred
906 adaptive diversification and speciation in a cosmopolitan bird clade. *Proceedings of the Royal*
907 *Society B*, 288(1958), 20211022. <https://doi.org/10.1098/rspb.2021.1022>

908 Law, R., Dixon-Salazar, T., Jerber, J., Cai, N., Abbasi, A. A., Zaki, M. S., ... & Gleeson, J. G. (2014). Biallelic
909 truncating mutations in FMN2, encoding the actin-regulatory protein Formin 2, cause
910 nonsyndromic autosomal-recessive intellectual disability. *The American Journal of Human*
911 *Genetics*, 95(6), 721-728. <https://doi.org/10.1016/j.ajhg.2014.10.016>

912 Lehti, M. S., Henriksson, H., Rummukainen, P., Wang, F., Uusitalo-Kylmä, L., Kiviranta, R., Heino, T. J.,
913 Kotaja, N., & Sironen, A. (2018). Cilia-related protein SPEF2 regulates osteoblast differentiation.
914 *Scientific Reports*, 8(1), 1–11. <https://doi.org/10.1038/s41598-018-19204-5>

915 Leroy, T., Rousselle, M., Tilak, M. K., Caizergues, A. E., Scornavacca, C., Recuerda, M., Fuchs, J., Illera, J.
916 C., De Swardt, D. H., Blanco, G., Thébaud, C., Milá, B., & Nabholz, B. (2021). Island songbirds as
917 windows into evolution in small populations. *Current Biology*, 31(6), 1303-1310.e4.
918 <https://doi.org/10.1016/j.cub.2020.12.040>

919 Li, H., & Durbin, R. (2009). Fast and accurate short read alignment with Burrows–Wheeler transform.
920 *Bioinformatics*, 26(5), 589–595. <https://doi.org/10.1093/bioinformatics/btp698>

921 Li, H., & Durbin, R. (2011). Inference of human population history from individual whole-genome
922 sequences. *Nature*, 475(7357), 493–496. <https://doi.org/10.1038/nature10231>

923 Li, H., Handsaker, B., Wysoker, A., Fennell, T., Ruan, J., Homer, N., Marth, G., Abecasis, G., & Durbin, R.
924 (2009). The sequence alignment/map format and SAMtools. *Bioinformatics*, 25(16), 2078–2079.
925 <https://doi.org/10.1093/bioinformatics/btp352>

926 Li, H., & Ralph, P. (2019). Local PCA shows how the effect of population structure differs along the
927 genome. *Genetics*, 211(1), 289–304. <https://doi.org/10.1534/genetics.118.301747>

928 Liu, X., Li, Y. I., & Pritchard, J. K. (2019). Trans effects on gene expression can drive omnigenic
929 inheritance. *Cell*, 177(4), 1022-1034.e6. <https://doi.org/10.1016/j.cell.2019.04.014>

930 Losos, J. B., & Ricklefs, R. E. (2009). Adaptation and diversification on islands. *Nature*, 457(7231), 830–
931 836. <https://doi.org/10.1038/nature07893>

932 Lovell, P. V., Clayton, D. F., Replogle, K. L., & Mello, C. V. (2008). Birdsong “transcriptomics”:
933 Neurochemical specializations of the oscine song system. *PLoS ONE*, 3(10), e3440.
934 <https://doi.org/10.1371/journal.pone.0003440>

935 Manceau, M., Domingues, V. S., Linnen, C. R., Rosenblum, E. B., & Hoekstra, H. E. (2010). Convergence in
936 pigmentation at multiple levels: Mutations, genes and function. *Philosophical Transactions of the*
937 *Royal Society B: Biological Sciences*, 365(1552), 2439–2450.
938 <https://doi.org/10.1098/rstb.2010.0104>

939 Marçais, G., Delcher, A. L., Phillippy, A. M., Coston, R., Salzberg, S. L., & Zimin, A. (2018). MUMmer4: A
940 fast and versatile genome alignment system. *PLoS Computational Biology*, 14(1), 1–14.
941 <https://doi.org/10.1371/journal.pcbi.1005944>

942 McVean, G., & Auton, A. (2007). LDhat 2.1: a package for the population genetic analysis of
943 recombination. *Department of Statistics, Oxford, OX1 3TG, UK*.
944 www.stats.ox.ac.uk/~mcvean/LDhat.html

945 Meier, J. I., Marques, D. A., Wagner, C. E., Excoffier, L., & Seehausen, O. (2018). Genomics of parallel
946 ecological speciation in Lake Victoria cichlids. *Molecular Biology and Evolution*, 35(6), 1489-1506.
947 <https://doi.org/10.1093/molbev/msy051>

948 Milá, B., Wayne, R. K., & Smith, T. B. (2008). Ecomorphology of migratory and sedentary populations of
949 the Yellow-rumped warbler (*Dendroica coronata*). *The Condor*, 110(2), 335–344.
950 <https://doi.org/10.1525/cond.2008.8396>

951 Møller, A. P. (2006). Sociality, age at first reproduction and senescence: comparative analyses of birds.
952 *Journal of Evolutionary Biology*, 19(3), 682–689. <https://doi.org/10.1111/j.1420-9101.2005.01065.x>

953 Moloney, G. M., van Oeffelen, W. E. P. A., Ryan, F. J., van de Wouw, M., Cowan, C., Claesson, M. J.,
954 Schellekens, H., Dinan, T. G., & Cryan, J. F. (2019). Differential gene expression in the
955 mesocorticolimbic system of innately high- and low-impulsive rats. *Behavioural Brain Research*,
956 364, 193–204. <https://doi.org/10.1016/j.bbr.2019.01.022>

957 Monroe, J., Srikant, T., Carbonell-Bejerano, P., Becker, C., Lensink, M., Exposito-Alonso, M., ... & Weigel,

958 D. (2022). Mutation bias reflects natural selection in *Arabidopsis thaliana*. *Nature* 602, 101-105.
959 <https://doi.org/10.1038/s41586-021-04269-6>

960 Morinha, F., Milá, B., Fargallo, J. A. ., & Blanco, G. (2020). The ghost of connections past: a role for
961 mainland vicariance in the isolation of an insular population of the red-billed chough (Aves:
962 Corvidae) *Journal of Biogeography* 47 (12), 2567-2583 <https://doi.org/10.1111/jbi.13977>.

963 Morris, S. C. (2010). Evolution: Like any other science it is predictable. *Philosophical Transactions of the*
964 *Royal Society B: Biological Sciences*, 365(1537), 133–145. <https://doi.org/10.1098/rstb.2009.0154>

965 Nachman, M. W., & Payseur, B. A. (2012). Recombination rate variation and speciation: Theoretical
966 predictions and empirical results from rabbits and mice. *Philosophical Transactions of the Royal*
967 *Society B: Biological Sciences*, 367(1587), 409–421. <https://doi.org/10.1098/rstb.2011.0249>

968 Nadachowska-Brzyska, K., Burri, R., Smeds, L., & Ellegren, H. (2016). PSMC analysis of effective
969 population sizes in molecular ecology and its application to black-and-white *Ficedula* flycatchers.
970 *Molecular Ecology*, 25(5), 1058–1072. <https://doi.org/10.1111/mec.13540>

971 Nadeau, N. J., Whibley, A., Jones, R. T., Davey, J. W., Dasmahapatra, K. K., Baxter, S. W., Quail, M. A.,
972 Joron, M., Ffrench-Constant, R. H., Blaxter, M. L., Mallet, J., & Jiggins, C. D. (2012). Genomic islands
973 of divergence in hybridizing *Heliconius* butterflies identified by large-scale targeted sequencing.
974 *Philosophical Transactions of the Royal Society B: Biological Sciences*. 367(1587), 343–353.
975 <https://doi.org/10.1098/rstb.2011.0198>

976 Nosil, P., Funk, D. J., & Ortiz-Barrientos, D. (2009). Divergent selection and heterogeneous genomic
977 divergence. *Molecular Ecology*. 18(3), 375-402. <https://doi.org/10.1111/j.1365-294X.2008.03946.x>

978 Oikkonen, J., Onkamo, P., Järvelä, I., & Kanduri, C. (2016). Convergent evidence for the molecular basis
979 of musical traits. *Scientific Reports*, 6(1), 1–10. <https://doi.org/10.1038/srep39707>

980 Osogwa, N. C., Mori, C, Sánchez-Valpuesta, M., Hayase, S. & Wada, K. (2018). Inter- and intra-species
981 differences in muscarinic acetylcholine receptor expression in the neural pathways for vocal
982 learning in songbirds. *The Journal of Comparative Neurology* 526(17) 2856-2869.
983 <https://doi.org/10.1002/cne.24532>.

984 Poelstra, J. W., Vijay, N., Bossu, C. M., Lantz, H., Ryll, B., Müller, I., Baglione, V., Unneberg, P., Wikelski,
985 M., Grabherr, M. G., & Wolf, J. B. W. (2014). The genomic landscape underlying phenotypic
986 integrity in the face of gene flow in crows. *Science*, 344(6190), 1410–1414.
987 <https://doi.org/10.1126/science.1253226>

988 Power, D. (1983). Variability in island populations of the house finch. *The Auk*, 100(1), 180–187.
989 <https://doi.org/10.1093/auk/100.1.180>

990 Price, T. (2008). *Speciation in birds*. Roberts and Company, CO.

991 Price, T. D., Grant, P. R., Gibbs, H. L., & Boag, P. T. (1984). Recurrent patterns of natural selection in a
992 population of Darwin's finches. *Nature*, 309(5971), 787–789. <https://doi.org/10.1038/309787a0>

993 Pritchard, J. K., & Di Rienzo, A. (2010). Adaptation - Not by sweeps alone. *Nature Reviews Genetics*,
994 11(10), 665–667. <https://doi.org/10.1038/nrg2880>

995 Qi, L. M., Mohr, M., & Wade, J. (2012). Enhanced expression of tubulin-specific chaperone protein α ,
996 mitochondrial ribosomal protein S27, and the DNA excision repair protein XPACCH in the song
997 system of juvenile male zebra finches. *Developmental Neurobiology*, 72(2), 199–207.
998 <https://doi.org/10.1002/dneu.20956>

999 Rappaport, N., Twik, M., Plaschkes, I., Nudel, R., Iny Stein, T., Levitt, J., Gershoni, M., Morrey, C. P.,
1000 Safran, M., & Lancet, D. (2017). MalaCards: an amalgamated human disease compendium with
1001 diverse clinical and genetic annotation and structured search. *Nucleic Acids Research*, 45(D1),
1002 D877-D887.

1003 Ravinet, M., Faria, R., Butlin, R. K., Galindo, J., Bierne, N., Rafajlović, M., Noor, M. A. F., Mehlig, B., &
1004 Westram, A. M. (2017). Interpreting the genomic landscape of speciation: a road map for finding
1005 barriers to gene flow. *Journal of Evolutionary Biology*, 30(8), 1450–1477.
1006 <https://doi.org/10.1111/jeb.13047>

1007 Recuerda, M., Illera, J. C., Blanco, G., Zardoya, R., & Milá, B. (2021). Sequential colonization of oceanic
1008 archipelagos led to a species-level radiation in the common chaffinch complex (Aves : *Fringilla*
1009 *coelebs*). *Molecular Phylogenetics and Evolution*, 164, 107291.
1010 <https://doi.org/10.1016/j.ympev.2021.107291>

1011 Recuerda, M., Vizueta, J., Cuevas-Caballé, C., Blanco, G., Rozas, J., & Milá, B. (2021). Chromosome-Level
1012 Genome Assembly of the Common Chaffinch (Aves: *Fringilla coelebs*): A Valuable Resource for
1013 Evolutionary Biology. *Genome Biology and Evolution*, 13(4), 1–6.
1014 <https://doi.org/10.1093/gbe/evab034>

1015 Reed, R. D., Papa, R., Martin, A., Hines, H. M., Counterman, B. A., Pardo-Diaz, C., ... & McMillan, W. O.
1016 (2011). Optix drives the repeated convergent evolution of butterfly wing pattern
1017 mimicry. *Science*, 333(6046), 1137-1141.

1018 Reid, J. M., Bignal, E. M., Bignal, S., McCracken, D. I., & Monaghan, P. (2003). Age-specific reproductive
1019 performance in red-billed choughs *Pyrhacorax pyrrhacorax*: Patterns and processes in a natural
1020 population. *Journal of Animal Ecology*, 72(5), 765–776. [https://doi.org/10.1046/j.1365-](https://doi.org/10.1046/j.1365-2656.2003.00750.x)
1021 [2656.2003.00750.x](https://doi.org/10.1046/j.1365-2656.2003.00750.x)

1022 Ren, S., Lyu, G., Irwin, D. M., Liu, X., Feng, C., Luo, R., Zhang, J., Sun, Y., Shang, S., Zhang, S., & Wang, Z.
1023 (2021). Pooled sequencing analysis of geese (*Anser cygnoides*) reveals genomic variations
1024 associated with feather color. *Frontiers in Genetics*, *12*, 650013.
1025 <https://doi.org/10.3389/fgene.2021.650013>

1026 Rising, J., & Somers, K. (1989). The measurement of overall body size in birds. *The Auk*, *106*(4), 666–674.
1027 <https://doi.org/10.1093/auk/106.4.666>

1028 Rosenblum, E. B., Parent, C. E., & Brandt, E. E. (2014). The molecular basis of phenotypic convergence.
1029 *Annual Review of Ecology, Evolution, and Systematics*, *45*, 203–226.
1030 <https://doi.org/10.1146/annurev-ecolsys-120213-091851>

1031 Sabeti, P. C., Varilly, P., Fry, B., Lohmueller, J., Hostetter, E., Cotsapas, C., ... & Lander, E. S. (2007).
1032 Genome-wide detection and characterization of positive selection in human
1033 populations. *Nature*, *449*(7164), 913–918. <https://doi.org/10.1038/nature06250>

1034 Sackton, T. B., & Clark, N. (2019). Convergent evolution in the genomics era: new insights and directions.
1035 *Philosophical Transactions of the Royal Society B: Biological Sciences*, *374*(1777), 24–27.
1036 <https://doi.org/10.1098/rstb.2019.0102>

1037 Sato, Y. U., Ogden, R., Kishida, T., Nakajima, N., Maeda, T., & Inoue-Murayama, M. (2020). Population
1038 history of the golden eagle inferred from whole-genome sequencing of three of its subspecies.
1039 *Biological Journal of the Linnean Society*, *XX*, 1–13.
1040 <https://doi.org/10.1093/biolinnean/blaa068/5865777>

1041 Sayol, F., Downing, P. A., Iwaniuk, A. N., Maspons, J., & Sol, D. (2018). Predictable evolution towards
1042 larger brains in birds colonizing oceanic islands. *Nature Communications*, *9*(1).
1043 <https://doi.org/10.1038/s41467-018-05280-8>

1044 Schluter, D. (2000). *The ecology of adaptive radiation*. OUP Oxford.

1045 Seehausen, O., Butlin, R. K., Keller, I., Wagner, C. E., Boughman, J. W., Hohenlohe, P. A., ... & Widmer, A.
1046 (2014). Genomics and the origin of species. *Nature Reviews Genetics*, *15*(3), 176–192.
1047 <https://doi.org/10.1038/nrg3644>

1048 Senar, J. C., & Pascual, J. (1997). Keel and tarsus length may provide a good predictor of avian body size.
1049 *Ardea*, *85*(2), 269–274.

1050 Sendell-Price, A. T., Ruegg, K. C., Robertson, B. C., & Clegg, S. M. (2021). An island-hopping bird reveals
1051 how founder events shape genome-wide divergence. *Molecular Ecology*, *30*(11), 2495–2510.

1052 Shi, Z., Zhang, Z., Schaffer, L., Huang, Z., Fu, L., Head, S., Gaasterland, T., Wang, X., & Li, X. (2021).
1053 Dynamic transcriptome landscape in the song nucleus HVC between juvenile and adult zebra

1054 finches. *Advanced Genetics*, 2(1), 1–13. <https://doi.org/10.1002/ggn2.10035>

1055 Shultz, A. J., Baker, A. J., Hill, G. E., Nolan, P. M., & Edwards, S. V. (2016). SNPs across time and space:
1056 population genomic signatures of founder events and epizootics in the House Finch (*Haemorhous*
1057 *mexicanus*). *Ecology and Evolution*, 6(20), 7475–7489. <https://doi.org/10.1002/ece3.2444>

1058 Singhal, S., Leffler, E. M., Sannareddy, K., Turner, I., Venn, O., Hooper, D. M., ... & Przeworski, M. (2015).
1059 Stable recombination hotspots in birds. *Science*, 350(6263), 928–932.
1060 <https://doi.org/10.1126/science.aad0843>

1061 Smeds, L., Qvarnström, A., & Ellegren, H. (2016). Direct estimate of the rate of germline mutation in a
1062 bird. *Genome Research*, 26(9), 1211–1218. <https://doi.org/10.1101/gr.204669.116>

1063 Steiner, C. C., Römpler, H., Boettger, L. M., Schöneberg, T., & Hoekstra, H. E. (2009). The genetic basis of
1064 phenotypic convergence in beach mice: Similar pigment patterns but different genes. *Molecular*
1065 *Biology and Evolution*, 26(1), 35–45. <https://doi.org/10.1093/molbev/msn218>

1066 Tajima, F. (1989). Statistical method for testing the neutral mutation hypothesis by DNA polymorphism.
1067 *Genetics*, 123(3), 585–595. <https://doi.org/PMC1203831>

1068 Tattersall, G. J., Arnaout, B., & Symonds, M. R. E. (2017). The evolution of the avian bill as a
1069 thermoregulatory organ. *Biological Reviews*, 92(3), 1630–1656. <https://doi.org/10.1111/brv.12299>

1070 Tattersall, G. J., Chaves, J. A., & Danner, R. M. (2018). Thermoregulatory windows in Darwin’s finches.
1071 *Functional Ecology*, 32(2), 358–368. <https://doi.org/10.1111/1365-2435.12990>

1072 Team, R. C. (2017). R: A language and environment for statistical computing. *R Foundation for Statistical*
1073 *Computing, Vienna, Austria*. URL <https://www.R-Project.Org>.

1074 Turner, S. D. (2018). qqman: an R package for visualizing GWAS results using Q-Q and manhattan plots.
1075 *Journal of Open Source Software*, 3(25), 731. <https://doi.org/10.21105/joss.00731>

1076 Turner, T. L., Hahn, M. W., & Nuzhdin, S. V. (2005). Genomic islands of speciation in *Anopheles gambiae*.
1077 *PLoS Biology*, 3(9), 1572–1578. <https://doi.org/10.1371/journal.pbio.0030285>

1078 Tuttle, E. M., Bergland, A. O., Korody, M. L., Brewer, M. S., Newhouse, D. J., Minx, P., Stager, M., Betuel,
1079 A., Cheviron, Z. A., Warren, W. C., Gonser, R. A., & Balakrishnan, C. N. (2016). Divergence and
1080 functional degradation of a sex chromosome-like supergene. *Current Biology*, 26(3), 344–350.
1081 <https://doi.org/10.1016/j.cub.2015.11.069>

1082 Van Doren, B. M., Campagna, L., Helm, B., Illera, J. C., Lovette, I. J., & Liedvogel, M. (2017). Correlated
1083 patterns of genetic diversity and differentiation across an avian family. *Molecular Ecology*, 26(15),
1084 3982–3997. <https://doi.org/10.1111/mec.14083>

1085 Vijay, N., Bossu, C. M., Poelstra, J. W., Weissensteiner, M. H., Suh, A., Kryukov, A. P., & Wolf, J. B. W.

1086 (2016). Evolution of heterogeneous genome differentiation across multiple contact zones in a crow
1087 species complex. *Nature Communications*, 7(1), 1–10. <https://doi.org/10.1038/ncomms13195>

1088 Vijay, N., Weissensteiner, M., Burri, R., Kawakami, T., Ellegren, H., & Wolf, J. B. W. (2017). Genomewide
1089 patterns of variation in genetic diversity are shared among populations, species and higher-order
1090 taxa. *Molecular Ecology*, 26(16), 4284–4295. <https://doi.org/10.1111/mec.14195>

1091 Vujovic, D., Cornblath, D. R., & Scherer, S. S. (2021). A recurrent MORC2 mutation causes Charcot-Marie-
1092 Tooth disease type 2Z. *Journal of the Peripheral Nervous System*, 26(2), 184–186.
1093 <https://doi.org/10.1111/jns.12443>

1094 Warren, B. H., Simberloff, D., Ricklefs, R. E., Aguilée, R., Condamine, F. L., Gravel, D., ... & Thébaud, C.
1095 (2015). Islands as model systems in ecology and evolution: Prospects fifty years after MacArthur-
1096 Wilson. *Ecology Letters*, 18(2), 200–217. <https://doi.org/10.1111/ele.12398>

1097 Weir, B. S., & Cockerham, C. C. (1984). Estimating F-Statistics for the Analysis of Population Structure.
1098 *Evolution*, 38(6), 1358–1370. <https://doi.org/10.2307/2408641>

1099 Whittaker, R. J., Fernández-Palacios, J. M., Matthews, T. J., Borregaard, M. K., & Triantis, K. A. (2017).
1100 Island biogeography: Taking the long view of nature's laboratories. *Science*, 357(6354), eaam8326.
1101 <https://doi.org/10.1126/science.aam8326>

1102 Wittkopp, P. J., Williams, B. L., Selegue, J. E., & Carroll, S. B. (2003). *Drosophila* pigmentation evolution:
1103 Divergent genotypes underlying convergent phenotypes. *Proceedings of the National Academy of
1104 Sciences of the United States of America*, 100(4), 1808–1813.
1105 <https://doi.org/10.1073/pnas.0336368100>

1106 Woolfit, M., & Bromham, L. (2005). Population size and molecular evolution on islands. *Proceedings of
1107 the Royal Society B: Biological Sciences*, 272(1578), 2277–2282.
1108 <https://doi.org/10.1098/rspb.2005.3217>

1109 Yang, Y., Topol, L., Lee, H., & Wu, J. (2003). Wnt5a and Wnt5b exhibit distinct activities in coordinating
1110 chondrocyte proliferation and differentiation. *Development*, 130(5), 1003–1015.
1111 <https://doi.org/10.1242/dev.00324>

1112 Yap, C. C., & Winckler, B. (2012). Harnessing the power of the endosome to regulate neural
1113 development. *Neuron*, 74(3), 440–451. <https://doi.org/10.1016/j.neuron.2012.04.015>

1114 Yeaman, S. (2013). Genomic rearrangements and the evolution of clusters of locally adaptive loci.
1115 *Proceedings of the National Academy of Sciences of the United States of America*, 110(19), E1743-
1116 E1751. <https://doi.org/10.1073/pnas.1219381110>

1117 Zhang, G., Li, C., Li, Q., Li, B., Larkin, D. M., Lee, C., ... & Froman, D. P. (2014). Comparative genomics

1118 reveals insights into avian genome evolution and adaptation. *Science*, 346(6215), 1311-1320.
1119 <https://doi.org/10.1126/science.1251385>.

1120 Zheng, X., Levine, D., Shen, J., Gogarten, S. M., Laurie, C., & Weir, B. S. (2012). A high-performance
1121 computing toolset for relatedness and principal component analysis of SNP data. *Bioinformatics*,
1122 28(24), 3326–3328. <https://doi.org/10.1093/bioinformatics/bts606>

1123 Zinzow-Kramer, W. M., Horton, B. M., Mckee, C. D., Michaud, J. M., Tharp, G. K., Thomas, J. W., Tuttle, E.
1124 M., Yi, S., & Maney, D. L. (2015). Genes located in a chromosomal inversion are correlated with
1125 territorial song in white-throated sparrows. *Genes, Brain and Behavior*, 14(8), 641–654.
1126 <https://doi.org/10.1111/gbb.12252>

1127
1128

1129 **Tables**

1130

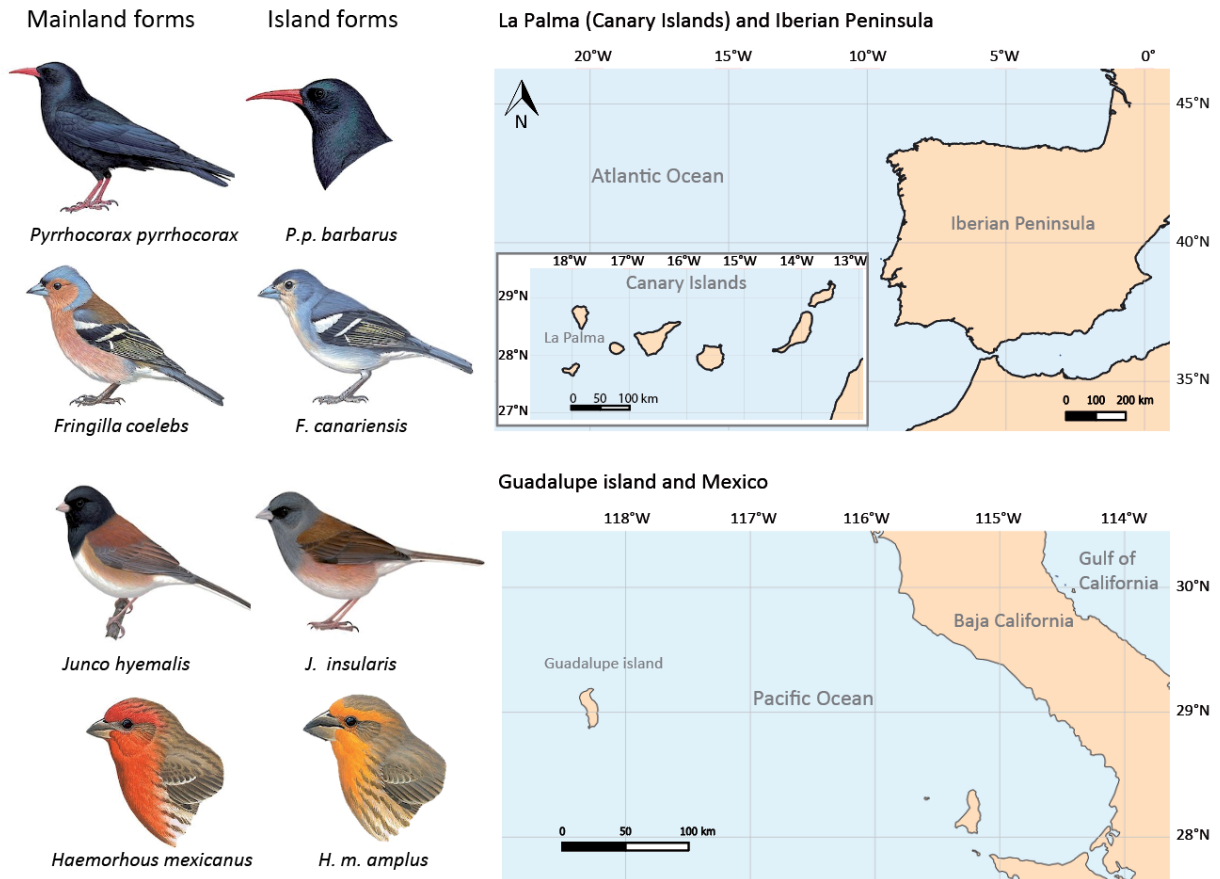
1131 **Table 1.** Divergence and diversity across the genome. Mean values, standard deviation and range of
 1132 genomic summary statistics for the four species, including: Samples sizes for the continental and insular
 1133 populations (N_{cont} and N_{is}), fixation Index (F_{ST}), absolute genomic divergence (d_{xy}), and genetic diversity
 1134 for the insular and the continental populations.

Species	N_{cont}	N_{is}	$F_{ST} \pm sd$	range	$d_{xy} \pm sd$	range	$\pi_{island} \pm sd$	range	$\pi_{continent} \pm sd$	range
Red-billed chough	12	12	0.21 ± 0.12	[-0.055 - 0.89]	0.0008 ± 0.0004	[0 - 0.15]	0.0005 ± 0.003	[0 - 0.013]	0.0008 ± 0.0004	[0 - 0.020]
House finch	12	12	0.14 ± 0.09	[-0.45 - 0.66]	0.006 ± 0.002	[0 - 0.017]	0.0043 ± 0.002	[0 - 0.018]	0.0052 ± 0.002	[0 - 0.016]
Dark-eyed junco	12	12	0.26 ± 0.07	[0.006 - 0.68]	0.005 ± 0.002	[0 - 0.023]	0.0022 ± 0.001	[0 - 0.023]	0.0049 ± 0.002	[0 - 0.022]
Common chaffinch	9	12	0.40 ± 0.05	[-0.033 - 0.88]	0.009 ± 0.003	[0 - 0.022]	0.0016 ± 0.001	[0 - 0.021]	0.0091 ± 0.003	[0 - 0.023]

1135

1136

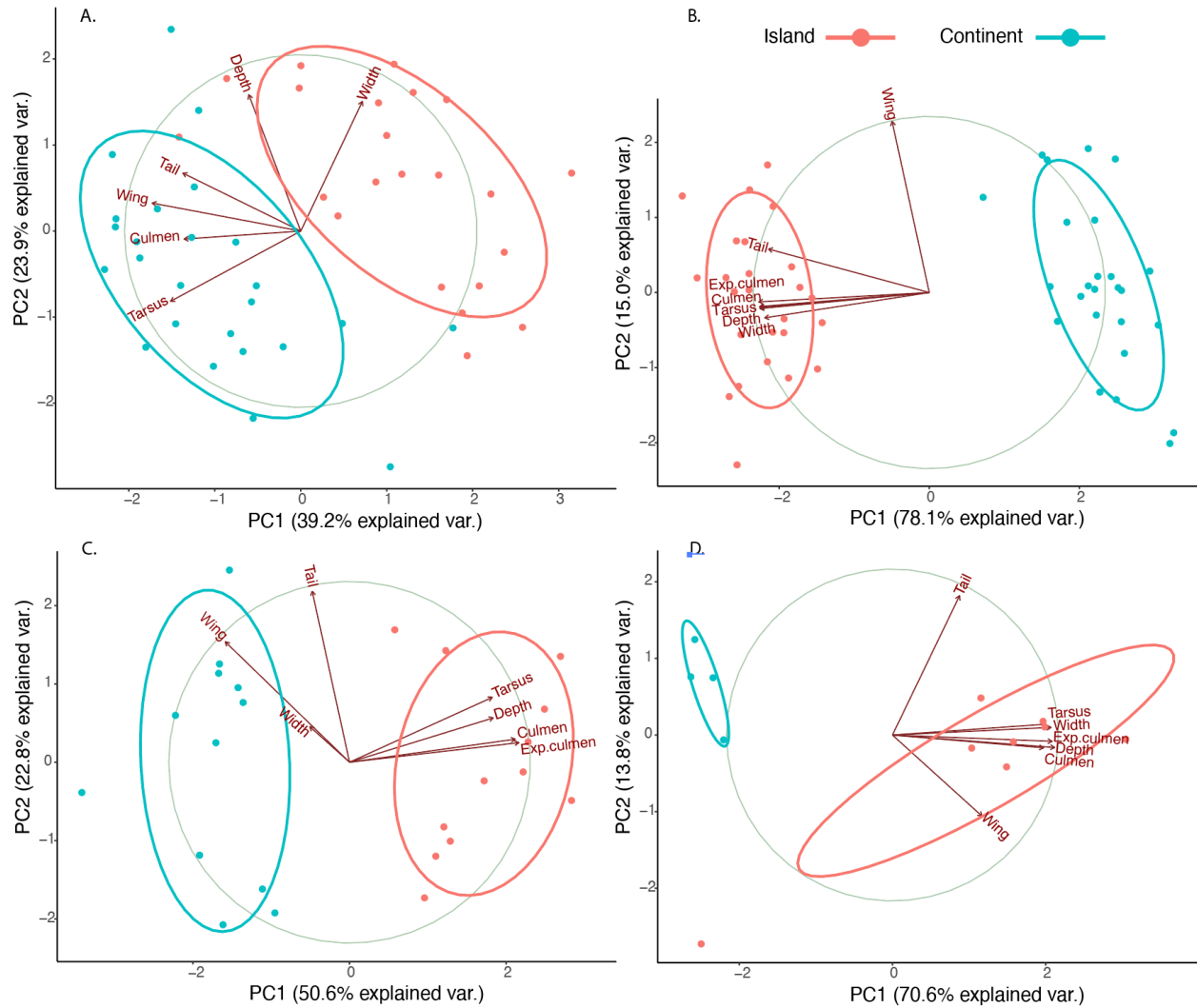
1137



1139

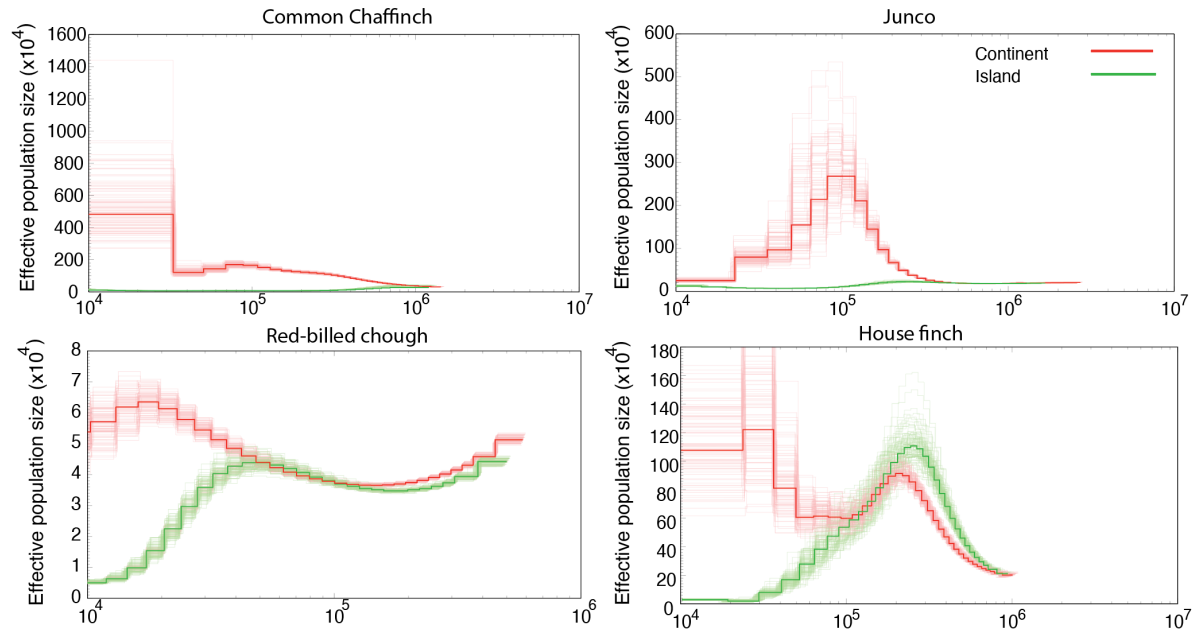
1140 **Figure 1. Target taxa for comparative analysis.** (A) Species that have colonized La Palma in the Atlantic
 1141 Ocean: the red-billed chough and the common chaffinch. (B) Species that have colonized Guadalupe
 1142 island in the Pacific Ocean: the dark-eyed junco and the house finch. Bird species according to Clements
 1143 et al., (2023). Bird illustrations from Billerman et al., (2022).

1144

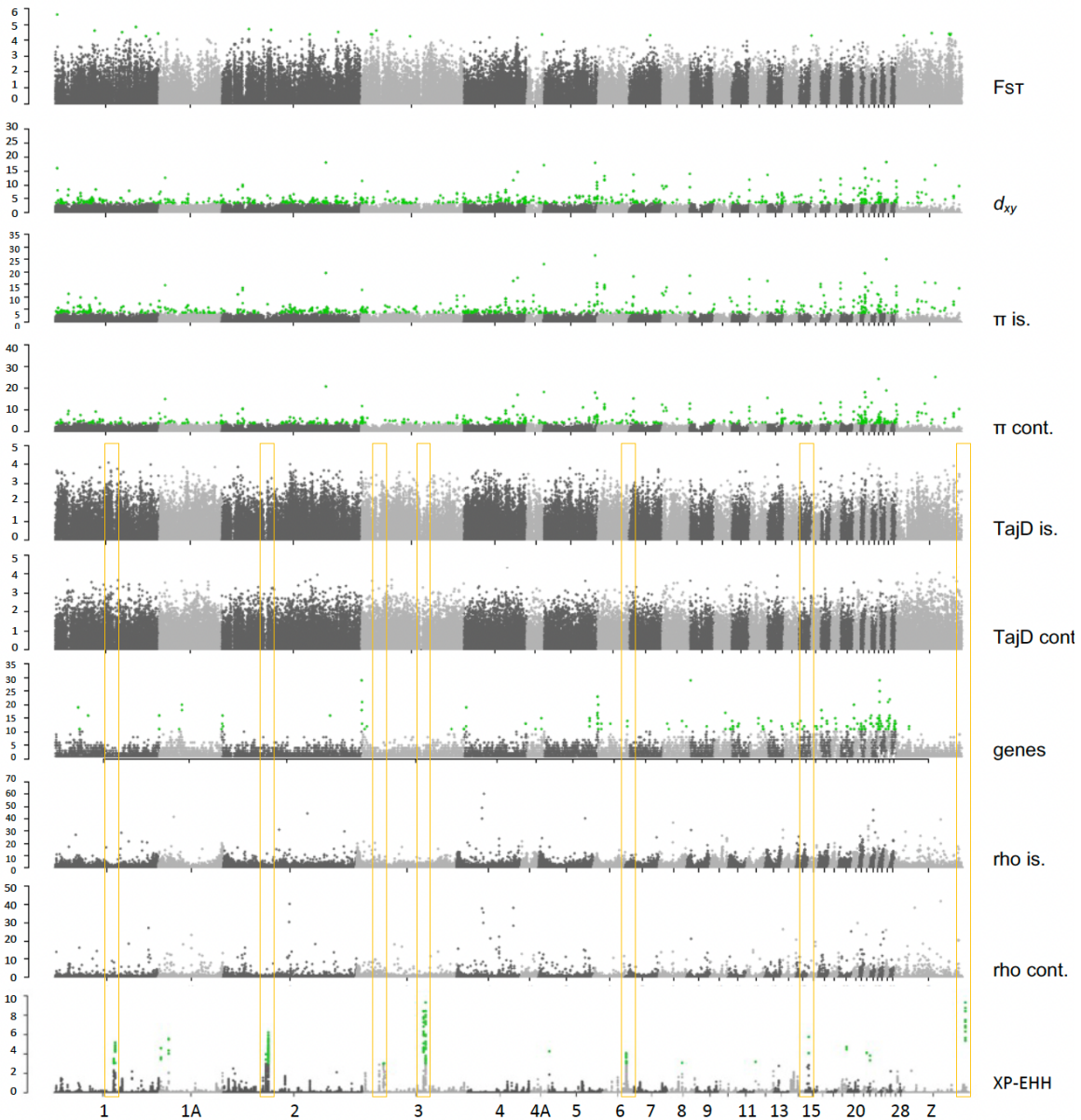


1145
 1146
 1147
 1148
 1149
 1150
 1151
 1152
 1153
 1154
 1155

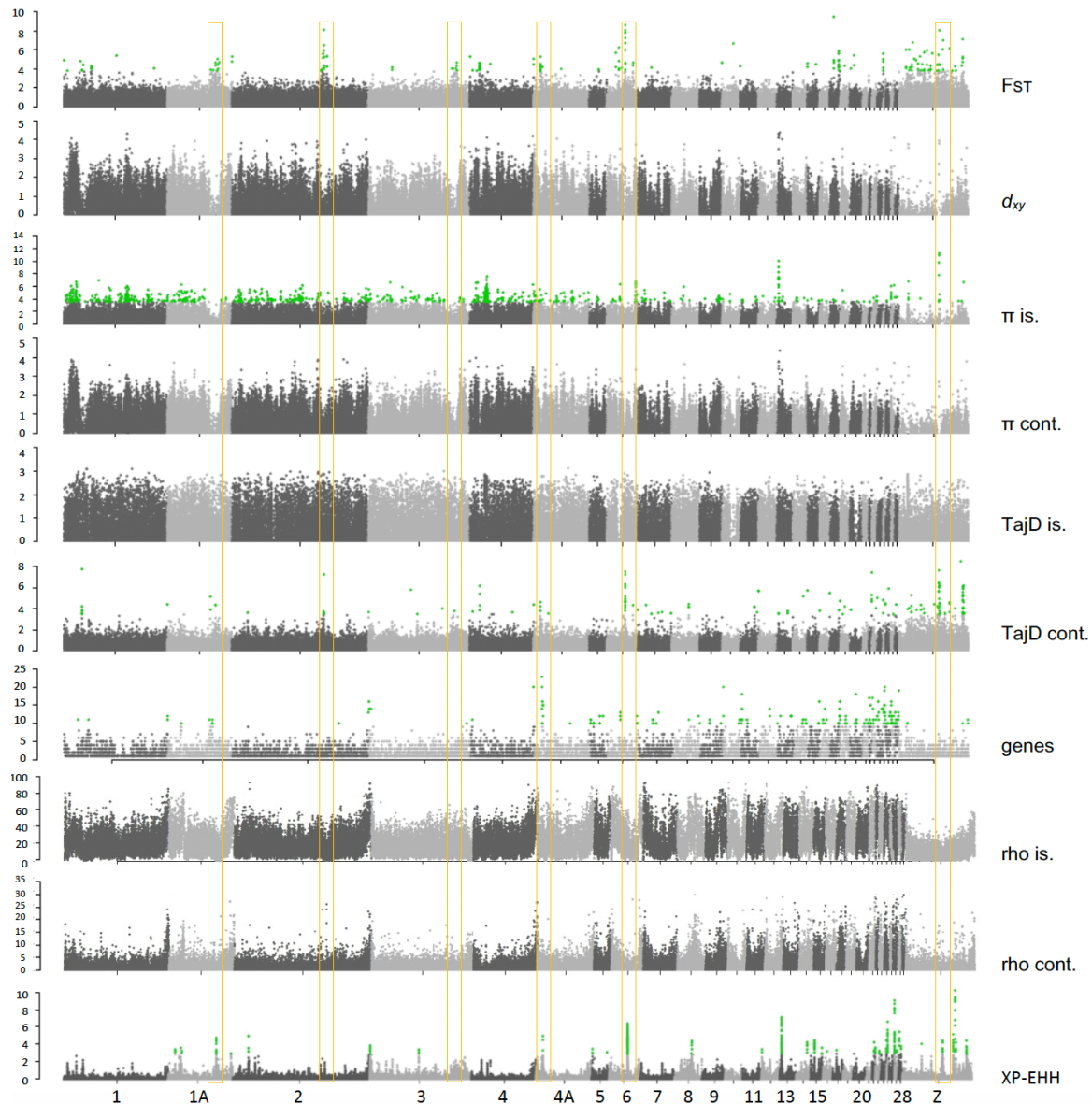
Figure 2. Principal Component Analysis (PCA) with morphological data per species A) Red-billed chough, B) Common/Canary Islands chaffinch, C) Dark-eyed/island junco, D) House finch. The variables included are wing, tail and tarsus length and bill depth, width, culmen and exposed culmen (the latter is not included for the red-billed chough). The correlation circle with radius 1 show the loadings of each variable that are represented by the arrows. The variables included are wing, tail and tarsus length and bill depth, width, culmen and exposed culmen (the latter is not included for the red-billed chough). Red and blue markers correspond to insular and mainland individuals, respectively.



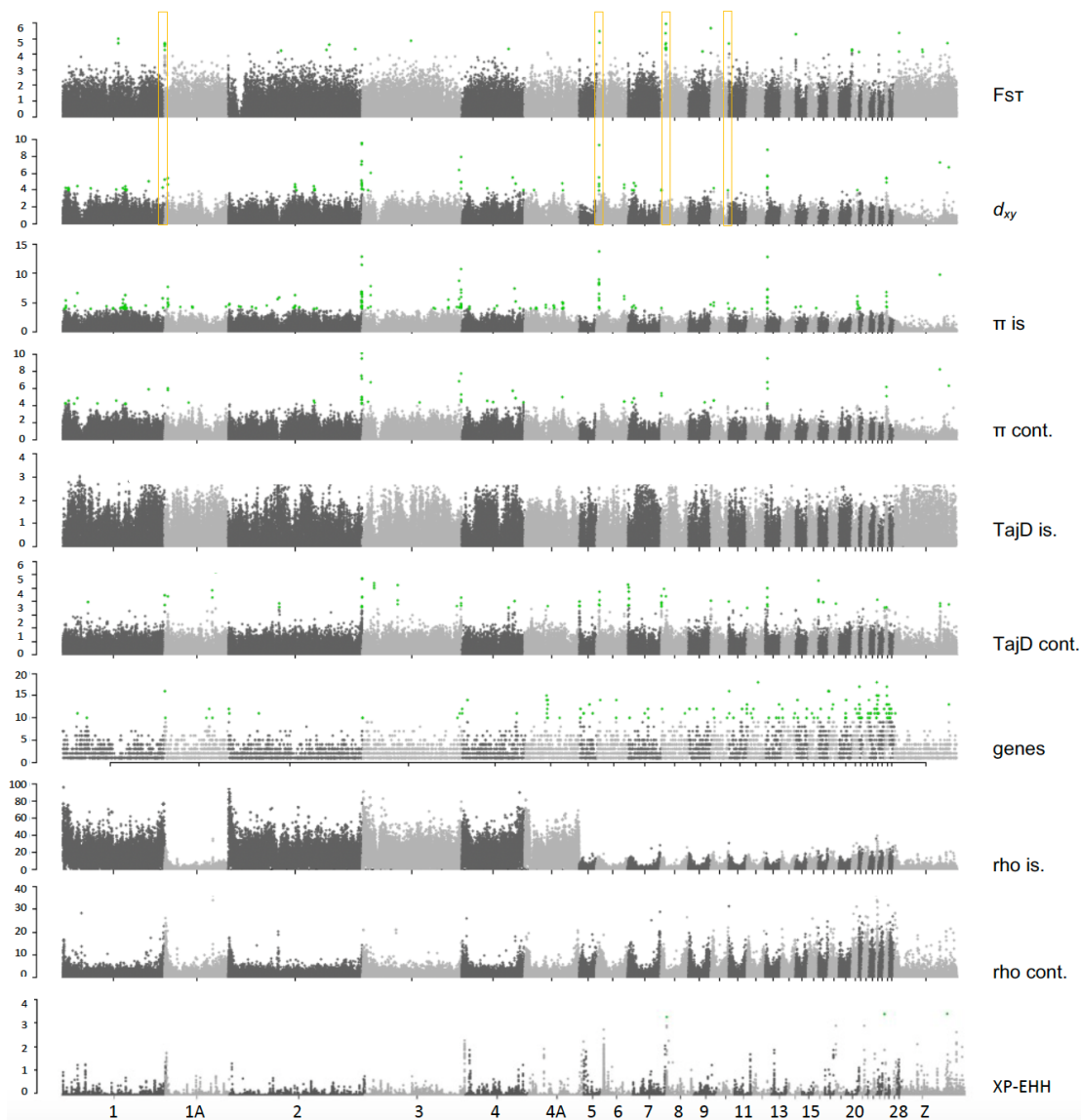
1156
 1157 **Figure 3.** Demographic history of insular and mainland populations. The analysis was performed using
 1158 Pairwise Sequentially Markovian Coalescent (PSMC). Demographic inference for one individual per
 1159 treatment and species, with the red and green dark lines corresponding to the continental and insular
 1160 populations, respectively. The lighter red and green lines represent 100 bootstrap replicates. The point
 1161 where both lines depart from each other corresponds to the time of colonization, which is around
 1162 40,000 y for the red-billed chough, 900,000 y for the common chaffinch, 100,000 y for the house finch
 1163 and 400,000 y for the dark-eye junco. The mutation rate used was of 4.6e-9 mutation/site/generation
 1164 for all species, and the generation time used in all cases was two years. See Fig. S2 for bootstrapped
 1165 versions of the individual PSMC plots.
 1166



1167
 1168 **Figure 4.** Genomic scans for several summary statistics for an island-mainland comparison in the red-
 1169 billed cough (*Pyrrhocorax pyrrhocorax*). From top to bottom, fixation index (F_{st}), genomic divergence
 1170 (d_{xy}), genetic diversity for insular and continental populations (π), Tajima's D for insular and continental
 1171 populations (TajD), number of genes, recombination rates for insular and mainland populations (rho)
 1172 and Cross-populations Extended Haplotype Homozygosity (XP-EHH). Chromosome numbers correspond
 1173 to the Zebra finch genome (*Taeniopygia guttata*). Green dots represent outliers with the false discovery
 1174 rate (FDR) set at 0.05 after applying the Benjamini and Hochberg correction, except for the XP-EHH,
 1175 where the threshold is set at $-\log_{10}(p\text{-value}) \geq 3$. The yellow boxes highlight the XP-EHH peaks
 1176 coincident with drops in Tajima's D.



1177
 1178 **Figure 5.** Genomic scans for several summary statistics for an island-mainland comparison in the
 1179 common chaffinch (*Fringilla coelebs*). From top to bottom, fixation index (F_{ST}), genomic divergence (d_{xy}),
 1180 genetic diversity for insular and continental populations (π), Tajima's D for insular and continental
 1181 populations (TajD), number of genes, recombination rates for insular and mainland populations (rho)
 1182 and Cross-populations Extended Haplotype Homozygosity (XP-EHH). Chromosome numbers correspond
 1183 to the Zebra finch genome (*Taeniopygia guttata*). Green dots represent outliers with the false discovery
 1184 rate (FDR) set at 0.05 after applying the Benjamini and Hochberg correction, except for the XP-EHH,
 1185 where the threshold is set at $-\log_{10}(p\text{-value}) \geq 3$. The yellow boxes highlight the signatures of recurrent
 1186 selection (F_{ST} peaks coincident with drops in d_{xy} and π). Some of them are also coincident with peaks in
 1187 XP-EHH.



1189

1190

1191

1192

1193

1194

1195

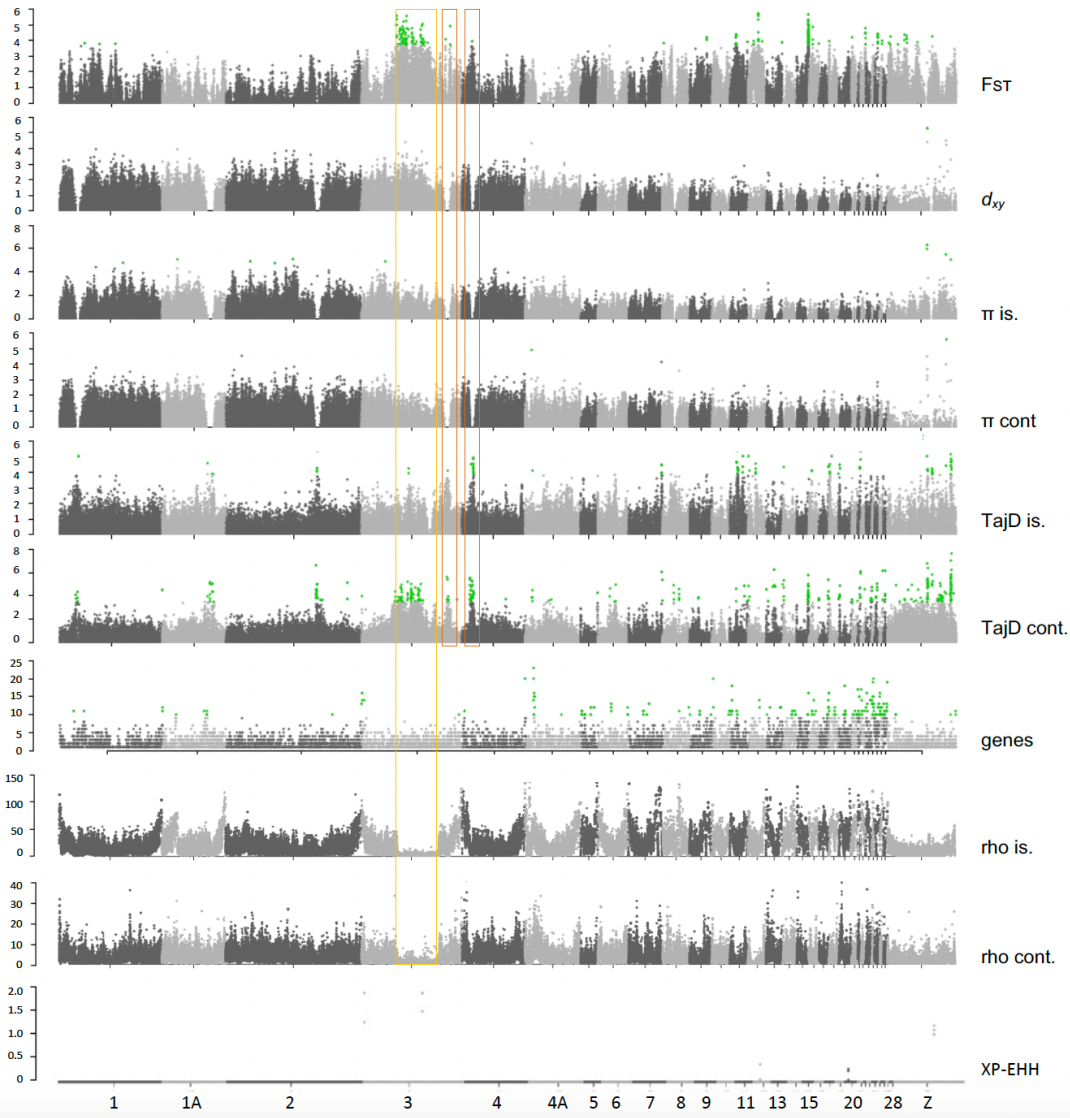
1196

1197

1198

1199

Figure 6. Genomic scans for several summary statistics for an island-mainland comparison in the dark-eyed junco (*Junco hyemalis*). From top to bottom, fixation index (F_{ST}), genomic divergence (d_{xy}), genetic diversity for insular and continental populations (π), Tajima's D for insular and continental populations (TajD), number of genes, recombination rates for insular and mainland populations (ρ) and Cross-populations Extended Haplotype Homozygosity (XP-EHH). Chromosome numbers correspond to the Zebra finch genome (*Taeniopygia guttata*). Green dots represent outliers with the false discovery rate (FDR) set at 0.05 after applying the Benjamini and Hochberg correction, except for the XP-EHH, where the threshold is set at $-\log_{10}(p\text{-value}) \geq 3$. The yellow boxes highlight the F_{ST} peaks in the chromosome extremes.



1200
 1201 **Figure 7.** Genomic scans for several summary statistics for an island-mainland comparison in the house
 1202 finch (*Haemorrhous mexicanus*). From top to bottom, fixation index (F_{ST}), genomic divergence (d_{xy}),
 1203 genetic diversity for insular and continental populations (π), Tajima's D for insular and continental
 1204 populations (TajD), number of genes, recombination rates por insular and mainland populations (rho)
 1205 and Cross-populations Extended Haplotype Homozygosity (XP-EHH). Chromosome numbers correspond
 1206 to the Zebra finch genome (*Taeniopygia guttata*). Green dots represent outliers with the false discovery
 1207 rate (FDR) set at 0.05 after applying the Benjamini and Hochberg correction, except for the XP-EHH,
 1208 where the threshold is set at $-\log_{10}(p\text{-value}) \geq 3$. The yellow box highlights the putative inversion in
 1209 chromosome 3 (F_{ST} peak that coincides with a drop in the recombination rate). The orange boxes
 1210 highlight the signatures of recurrent selection (F_{ST} peak coincident with drops in d_{xy} and π).